

**Study of the in-medium nucleon electromagnetic form factors
using a light-front nucleon wave function combined with the
quark-meson coupling model**

W. R. B. de Araújo^a, J. P. B. C. de Melo^b, K. Tsushima^b

^a *Secretaria de Educação do Estado de São Paulo,
DE Norte 2, São Paulo, SP, Brazil. and*

^b *Laboratório de Física Teórica e Computacional,
Universidade Cruzeiro do Sul, 01506-000, São Paulo, SP, Brazil*

(Dated: December 29, 2017)

Abstract

We study the nucleon electromagnetic (EM) form factors in symmetric nuclear matter as well as in vacuum within a light-front approach using the in-medium inputs calculated by the quark-meson coupling model. The same in-medium quark properties are used as those used for the study of in-medium pion properties. The zero of the proton EM form factor ratio in vacuum, the electric to magnetic form factor ratio $\mu_p G_{Ep}(Q^2)/G_{Mp}(Q^2)$ ($Q^2 = -q^2 > 0$ with q being the four-momentum transfer), is determined including the latest experimental data by implementing a hard constituent quark component in the nucleon wave function. A reasonable fit is achieved for the ratio $\mu_p G_{Ep}(Q^2)/G_{Mp}(Q^2)$ in vacuum, and we predict that the Q_0^2 value to cross the zero of the ratio to be about 15 GeV^2 . In addition the double ratio data of the proton EM form factors in ^4He and H nuclei, $[G_{Ep}^{4\text{He}}(Q^2)/G_{Mp}^{4\text{He}}(Q^2)]/[G_{Ep}^{\text{H}}(Q^2)/G_{Mp}^{\text{H}}(Q^2)]$, extracted by the polarized ($\vec{e}, e'\vec{p}$) scattering experiment on ^4He at JLab, are well described. We also predict that the Q_0^2 value satisfying $\mu_p G_{Ep}(Q_0^2)/G_{Mp}(Q_0^2) = 0$ in symmetric nuclear matter, shifts to a smaller value as increasing nuclear matter density, which reflects the facts that the faster falloff of $G_{Ep}(Q^2)$ as increasing Q^2 and the increase of the proton mean-square charge radius. Furthermore, we calculate the neutron EM form factor double ratio in symmetric nuclear matter for $0.1 < Q^2 < 1.0 \text{ GeV}^2$. The result shows that the neutron double ratio is enhanced relative to that in vacuum, while for the proton it is quenched, and agrees with an existing theoretical prediction.

PACS numbers: 24.85.+p, 21.65.-f, 14.20.Dh, 13.40.Gp, 12.39.-x

I. INTRODUCTION

One of the most challenging and exciting topics in hadronic and nuclear physics is how the hadron properties are modified in a nuclear medium (nuclear environment), and how such modifications can be measured in experiment. Since hadrons are composed of quarks, antiquarks and gluons, it is natural to expect that the hadron internal structure is modified when they are immersed in a nuclear medium and in atomic nuclei [1–7]. At sufficiently high nuclear density and/or temperature, there is no doubt that the quark and gluon degrees of freedom are the correct degrees of freedom to describe the properties of hadrons according to quantum chromodynamics (QCD). On the other hand, it is also true that effective description of hadronic and nuclear processes is very successful by means of the meson and baryon degrees of freedom, especially in a lower energy and temperature region. Although there is hope that lattice QCD simulation eventually can describe consistently the properties of hadrons in a nuclear medium as well as nucleus itself, the current status using physical pion mass value seems still difficult to get a reliable result at finite nuclear density [8–11].

To understand the deep inelastic scattering (DIS) data at momentum transfer of several GeV, one certainly needs explicit quark degrees of freedom [12–14]. In particular, the nuclear European Muon Collaboration (EMC) effect [15, 16] has suggested the necessity of including the degrees of freedom beyond the traditional nucleon and mesons. Furthermore, there is strong implication for the modifications of the bound proton electromagnetic (EM) form factors in the measurement of the double ratio of proton-recoil polarization transfer coefficients in $(\vec{e}, e'\vec{p})$ scattering experiments on ^{16}O and ^4He nuclei at MAMI and JLab [17–19]. It is also clear that the properties of bound neutron is modified in a nucleus, since it becomes stable, while the free neutron mean life is about 880 seconds due to the beta decay emitting a proton and an antineutrino [16, 20].

However, it is very difficult to unambiguously separate and identify the observed effects by the relevant degrees of freedom. In particular, to distinguish the possible in-medium modifications due to the nucleon internal structure change in a nuclear medium [2–7, 15, 16, 21–25], from those due to the conventional many-body effects, such as the final state interactions and meson exchange effects described at the hadronic degrees of freedom [26]. Such separation may only be possible in a model dependent manner, since general experimental data involve all the effects simultaneously. Thus, the interpretation of the modifications observed

in experiments has not yet been established.

In this article, we study the modifications of the nucleon EM form factors in symmetric nuclear matter, focusing on the internal structure change of nucleon. Namely, we study them based on the property change of the light-flavor (u and d) quarks inside the nucleon, using the in-medium inputs calculated by the quark-meson coupling (QMC) model [3, 4]. The purposes of the present study may be summarized as follows: (i) Since the interpretation of the medium modifications observed in experiments has not yet been established, one needs to study the issue by various different approaches/models to understand better, (ii) it is very interesting to study the effect of three-valence-quark-(spin)coupling to form the nucleon wave function, not by additive, independent quark models such models as in Refs. [3, 4, 21, 22, 24], (iii) a preliminary, similar study using the same model exists [25], but now we have the updated data for the proton EM form factors, and can study with the improved parameters for the nucleon wave function, especially improving the high Q^2 region behavior, (iv) the in-medium inputs in Ref. [25] were adapted from Ref. [23, 24] that based on the relativistic harmonic oscillator confining potential, however, it turned out that such approach cannot describe well the properties of finite nuclei without introducing nonlinear meson interaction terms at the meson and nucleon level Lagrangian [27]. Thus we tempt to use the in-medium inputs from the QMC model, which have successfully been applied for studying various nuclear and hadronic reactions as well as the properties of finite (hyper)nuclei, and (v) we calculate the in-medium neutron EM form factor double ratio in addition to that of the proton, which was predicted in Ref. [28] to be enhanced in medium contrary to the proton case, and demonstrate that our model result indeed agrees with the prediction. A similar approach as in the present study was already applied for the study of pion properties in symmetric nuclear matter [29–32]. Although there may be possible to have alternative explanations based on traditional nuclear physics approaches, our interest of this study is on the internal structure change of nucleon in a nuclear medium.

For this purpose, we rely on a light-front model of nucleon in vacuum, the “relativistic quark-spin coupling” model, which was used for studying the nucleon EM form factors [33, 34] as well as the nucleon EM and axial-vector [35] form factors in vacuum with some extensions including one of the present authors. Although we focus on the in-medium modifications of nucleon EM form factors in this study, the model could also describe reasonably well the axial-vector form factor and the coupling constant g_A (obtained values

$g_A = 1.09 - 1.29$) in vacuum with the quark mass values 330 – 380 MeV [35]. Note that, the present model corresponds to the parameter $\alpha = 1$ in the model of Ref. [35], and has an extra high-momentum component in the nucleon wave function. However, as studied in Refs. [33, 34], the introduction of the high-momentum component does not destroy the achieved good feature of the model in the lower Q^2 region, such as g_A at $Q^2 = 0$. For a smaller quark mass value such as 220 MeV to be used in this study, an exact calculation is planned to be performed in the near future. This model can keep close connection with covariant field theory, and perform a three-dimensional reduction for the photo-absorption amplitude with the nucleon projected on the null-plane, $x^+ = x^0 + x^3 = 0$. After the three-dimensional reduction, one can introduce the nucleon light-front wave function in the two-loop momentum integrations. For studying the nucleon EM form factors, the “triangle diagrams” with an impulse approximation is used. In Ref. [33] the hard-scale component in the nucleon wave function was firstly introduced to improve the description of the zero of the proton EM form factor ratio, $\mu_p G_{Ep}(Q^2)/G_{Mp}(Q^2)$ ($Q^2 = -q^2 > 0$, q the four-momentum transfer). In addition a detailed study was made for the different quark-spin coupling effects in Refs. [33, 34]. It turned out that the neutron electric form factor can strongly constrain the quark-spin coupling in the nucleon wave function, and the model preferred the scalar-pair coupling. Furthermore, to describe the zero of the proton EM form factor ratio, the introduction of the hard-scale component in the nucleon wave function was crucial. Thus, we use the two-scale model of the nucleon wave function in vacuum with the scalar-pair coupling, and study the medium modifications of the nucleon EM form factors, where the scalar-pair coupling means that, as will be given in Eq. (1), the coupling between the (three quarks)-nucleon coupling is made by the Lorentz scalar. Other possibilities of the couplings were also studied in Refs. [33–35]. Although it is also very interesting to study the medium effects on the nucleon axial-vector form factor within the same model, this is planned to be made in the near future.

We predict the Q_0^2 value to cross the zero of the ratio, $\mu_p G_{Ep}(Q_0^2)/G_{Mp}(Q_0^2) = 0$, to be about 15 GeV². Furthermore, the double ratio data of the proton EM form factors in ⁴He and H nuclei, $[G_{Ep}^{4\text{He}}(Q^2)/G_{Mp}^{4\text{He}}(Q^2)]/[G_{Ep}^{\text{H}}(Q^2)/G_{Mp}^{\text{H}}(Q^2)]$, extracted by the polarized ($\vec{e}, e'\vec{p}$) scattering experiment on ⁴He at JLab, turn out to be well described. We also predict the Q_0^2 value of $\mu_p G_{Ep}(Q_0^2)/G_{Mp}(Q_0^2) = 0$ in a nuclear medium, shifts to a smaller value as increasing nuclear matter density.

The organization of this article is as follows. In Sec. II, we explain the relativistic quark-spin coupling model of nucleon, two scale-model as well as the nucleon EM form factors in a light-front approach, and present the nucleon EM form factors in vacuum. In Sec. III we review the properties of nuclear medium necessary to study the in-medium modifications of the nucleon EM form factors, the QMC model, and discuss the in-medium inputs. We present main results of this study, the in-medium nucleon EM form factors in Sec. IV. Finally, we give summary and discussions in Sec. V.

II. NUCLEON ELECTROMAGNETIC FORM FACTORS IN VACUUM

Here, we briefly review a light-front approach for the nucleon structure, the relativistic quark-spin coupling model, and the two-scale model [33]. The effective Lagrangian for the quark-spin coupling in the nucleon [33–36], accounts for calculating the static EM observables with a totally symmetric momentum component of the nucleon wave function. However, the initial version of the model was necessary to be improved to describe better the zero of $\mu_p G_{Ep}(Q^2)/G_{Mp}(Q^2)$ [37–44], namely, the position of the zero to be shifted to a larger Q^2 . The effective Lagrangian for the three constituent quarks coupled to form the nucleon wave function is given by [33–36],

$$\mathcal{L}_{N-3q} = m_N \epsilon^{lmn} \bar{\Psi}_{(l)} i\tau_2 \gamma_5 \Psi_{(m)}^C \bar{\Psi}_{(n)} \Psi_N + H.C., \quad (1)$$

where τ_2 is the Pauli matrix operating in isospin space, and the color indices are $\{l, m, n\}$ with ϵ^{lmn} being the totally antisymmetric tensor. The conjugate quark field is $\Psi^C = C\bar{\Psi}^T$ with $C = i\gamma^2\gamma^0$, the charge conjugation matrix, and T stands for transposition. Quark flavor and spin quantum numbers are implicit in the quark field operators, and they will be treated properly when one calculates relevant matrix elements as was done in Refs. [33–36], and partly shown in Appendix A.

The momentum scale of the nucleon wave function for Gaussian and power law shapes with constituent up and down quark mass $m_q = 0.22$ GeV, was found to be about 0.6 - 0.8 GeV from the fit to the nucleon magnetic moments and mean-square charge radii [33]. (We note that the same value of the up and down quark constituent mass $m_q = 0.22$ GeV was also used for the studies of pion properties in vacuum [45], as well as in medium [29–32].) It turned out that the neutron electric form factor can constrain the relativistic quark-spin

coupling scheme, and the scalar-pair coupling in the effective Lagrangian is preferred.

However, although the effective Lagrangian approach to the quark-spin coupling allows a reasonable account for the static nucleon EM observables with a totally symmetric momentum component of the nucleon wave function, it has a too small momentum scale which leads to too small value for the zero of $\mu_p G_{Ep}(Q^2)/G_{Mp}(Q^2)$ [25, 33] than that the experimental data imply [37–44].

Therefore within this approach, one is led to introduce another term in the momentum component of the nucleon wave function, which would represent a higher-momentum scale, to be able to describe better the zero of $\mu_p G_{Ep}(Q^2)/G_{Mp}(Q^2)$ without destroying the good description achieved in the lower momentum transfer region [33, 34].

In some light-front models applied to mesons [46–53], a high-momentum scale appears naturally associated with the short-range interaction between the constituent quarks. A reasonable description of the meson spectrum and pion properties was achieved including a Dirac-delta interaction in the mass-squared operator [46–48], inspired by the hyperfine interaction from the effective one-gluon exchange between the constituent quarks [46, 54]. The model [48] reveals some of the physics contained in the observation of the trajectories of mesons in the (n, M^2) -plane, that are almost linear [55, 56]. The model naturally incorporates the small pion mass as a consequence of the short-range attraction in the spin-zero channel, which is also responsible for the pion and rho-meson mass splitting [48].

The short-range attractive part of the quark-quark interaction which is presented in the Godfrey and Isgur model [57], generates a high-momentum component as well in the light-cone pion wave function above the energy 1 GeV, and was successfully able to describe the electroweak structure of pion [58]. Nonetheless, it was pointed out that the existing electroweak data were not enough to draw a definite conclusion about the presence of the hard constituent-quark components in the hadron wave function [59]. Recently, this discussion led to a new insight when the valence-quark light-cone momentum distribution was probed in the experiment of diffractive dissociation of 500-GeV π^- into dijets [60], which supports the importance of the asymptotic part of the wave function [61], and the presence of a high-momentum component in the pion wave function [47].

Motivated by the above discussions which indicate the necessity of a strong short-range attractive interaction in the spin-zero channel and a high-momentum tail in the pion valence component in the wave function, we introduce a high-momentum component in the valence

nucleon wave function. We study the role of this high-momentum component in the calculation of the nucleon EM form factors. Indeed, the quality of the model description including the recent data for $\mu_p G_{Ep}(Q^2)/G_{Mp}(Q^2)$, is improved substantially as we show later.

Thus, we use the “two-scale model”, which includes the high-momentum component in the nucleon wave function in a light-front approach, in an effective Lagrangian with the spin coupling between the quarks Eq. (1) in a scalar form. Furthermore, we choose a power-law form [54, 62] for the momentum component of the nucleon wave function,

$$\Psi_{\text{Power}} = N_{\text{Power}} \left[(1 + M_0^2/\beta^2)^{-p} + \lambda(1 + M_0^2/\beta_1^2)^{-p} \right] , \quad (2)$$

$$\lambda = \left[(1 + M_H^2/\beta_1^2)/(1 + M_H^2/\beta^2) \right]^p , \quad (3)$$

which preserves the asymptotic behavior suggested by QCD. (See Eq. (A7) in Appendix A for the expression of M_0^2 .) The normalization constant N_{Power} above is determined by the proton charge. The characteristic momentum scales of the wave function are represented by β , β_1 and M_H , while M_0 is the free mass of the three-quark system, and its explicit expression is also given in Ref. [33]. The lower momentum scale is essentially determined by the nucleon static observables, while the higher one is related with the zero of $G_{Ep}(Q^2)$. A possible definition of the high-momentum scale brought by Eq. (2) is the value of M_0 at which the two terms are equal, therefore one easily gets,

$$\beta_H = \beta\beta_1 \left(\frac{1 - |\lambda|^{\frac{1}{3}}}{\beta_1^2 |\lambda|^{\frac{1}{3}} - \beta^2} \right)^{\frac{1}{2}} . \quad (4)$$

We stress that this value should be interpreted as a guiding reference. Note that the asymptotic behavior of Eq. (2) does not depend on the parameters. The totally symmetric forms of Eq. (2), due to the relativistic spin-coupling coefficients which depend on momentum, effectively lead to the breaking of the SU(6) flavor symmetry as discussed in Ref. [63].

The falloff based on perturbative QCD arguments for the power-law, has a value of $p = 3.5$ in Eq. (2) [54, 62]. From the point of view of the static electroweak observables, the value of p does not present an independent feature, once one static observable is fitted. Namely, the other parameters in Eq. (2) are strongly correlated, as long as $p > 2$ [33, 62]. In this study, we choose $p = 3$.

The light-front formulation of the nucleon electroweak form factors in Ref. [33] uses the effective Lagrangian Eq. (1), to construct the coupling of the quark spin in the valence

component of the nucleon wave function. The form factor calculation is made by an impulse approximation defined within a covariant field theory. The nucleon virtual photon absorption amplitude is projected on the three-dimensional hypersurface, $x^+ = x^0 + x^3 = 0$ (see, e.g., Ref. [64]).

The elimination of the relative light-front time between the particles in favor of the global time propagation [65–67], comes from the analytical integration in the individual light-front energies ($k^- = k^0 - k^3$) in the two-loop amplitude. Then, the momentum component of the nucleon light-front wave function is introduced into the remaining form of the two-loop three-dimensional momentum integrations which define the matrix elements of the electroweak currents [33, 66, 68].

The plus component of the nucleon EM current ($J_N^+ = J_N^0 + J_N^3$) for momentum transfers satisfying the Drell-Yan condition $q^+ = q^0 + q^3 = 0$, is used to calculate the EM form factors. The contribution of the Z-diagram is minimized in a Drell-Yan frame, while the wave function contribution to the current is maximized [54, 64, 66, 68, 69]. We use the Breit-frame, where the four-momentum transfer $q = (0, \vec{q}_\perp, 0)$ is such that ($q^+ = 0$) and $\vec{q}_\perp = (q^1, q^2)$, satisfying the Drell-Yan condition.

The nucleon EM form factors are calculated with the matrix elements of the current $J_N^+(Q^2)$ in the light-front spinor basis in the Breit-frame with the Drell-Yan condition [33, 70]. The Dirac and Pauli form factors are respectively given by,

$$\begin{aligned} F_{1N}(Q^2) &= \frac{1}{\sqrt{1+\eta}} \langle N \uparrow | J_N^+(Q^2) | N \uparrow \rangle , \\ F_{2N}(Q^2) &= \frac{1}{\sqrt{\eta}\sqrt{1+\eta}} \langle N \uparrow | J_N^+(Q^2) | N \downarrow \rangle , \end{aligned} \quad (5)$$

where $\eta = Q^2/4m_N$. The momentum transfer in the Breit-frame is chosen along the x-direction, i.e., $\vec{q}_\perp = (\sqrt{Q^2}, 0)$.

The nucleon electric and magnetic form factors (Sachs form factors) are given by:

$$\begin{aligned} G_{EN}(Q^2) &= F_{1N}(Q^2) - \frac{Q^2}{4m_N^2} F_{2N}(Q^2) , \\ G_{MN}(Q^2) &= F_{1N}(Q^2) + F_{2N}(Q^2) , \end{aligned} \quad (6)$$

with $N = p$ or n . $\mu_N = G_{MN}(0)$ is the magnetic moment and $\kappa_N = F_{2N}(0)$ is the anomalous one. The nucleon mean-square charge radius r_N^2 is calculated by $r_N^2 \equiv \langle r_N^2 \rangle = -6 \frac{dG_{EN}(Q^2)}{dQ^2} \Big|_{Q^2=0}$.

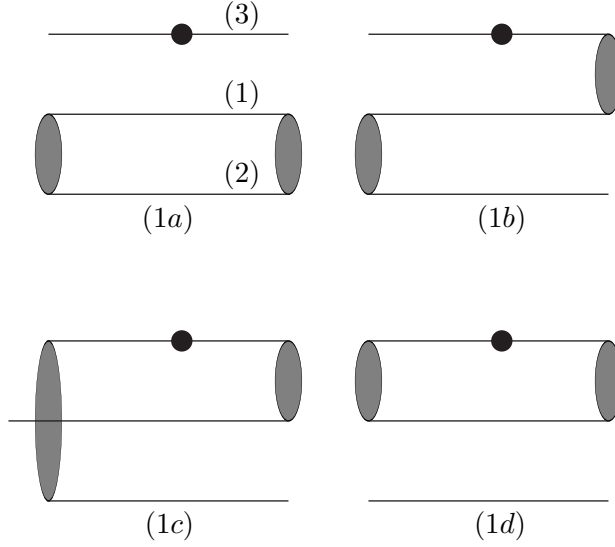


FIG. 1: Diagrammatic representation of the nucleon photo-absorption amplitude. The gray blob represents the spin invariant for the coupled quark pair in the effective Lagrangian Eq. (1). The small filled circle attached to the quark line represents the action of the EM current operator.

The microscopic matrix elements of the nucleon EM current are derived from the effective Lagrangian Eq. (1), within the light-front impulse approximation which is represented by four three-dimensional two-loop diagrams in Fig. 1 [33]. The diagrams embody the antisymmetrization of the quark state in the wave function. In all diagrams in Fig. 1, the quark 3 (the quark line with a small filled circle), is the quark which absorbs the momentum transfer by a photon. Figure (1a) [to be denoted by J_{aN}^+], defines the spin operator and represents the coupling between the quarks 1 and 2, while Fig. (1b) [to be denoted by J_{bN}^+], the coupled quarks in the nucleon initial state are the pair (1-3), and the coupled quarks in the nucleon final state are the pair (1-2). This current J_{bN}^+ represented by diagram (1b) should be multiplied by a factor 4 — a factor 2 comes from the exchange between the quarks 1 and 2, which are indistinguishable by this exchange, and the other factor 2 comes from the exchange between the pairs in the initial and final nucleon states, due the transformation

by the time reversal and parity. The process represented by figure (1c) [to be denoted by J_{cN}^+], where, in the initial state the coupled quarks are pair (1-3) and in the final state the coupled quarks are pair (2-3). This current should be multiplied by a factor 2, since the quarks 1 and 2 can be exchanged. The process represented by diagram (1d) [to be denoted by J_{dN}^+], corresponds to the process in which a photon is absorbed by the diquark formed by the quarks 1 and 3, while the quark 2 is the spectator. In this case we must multiply a factor 2 by possible exchange of the quarks 1 and 2. Therefore, the microscopic EM current operator for the nucleon depicted in Fig. 1 is given by,

$$J_N^+(Q^2) = J_{aN}^+(Q^2) + 4J_{bN}^+(Q^2) + 2J_{cN}^+(Q^2) + 2J_{dN}^+(Q^2), \quad (7)$$

with the factors explained. The explicit expressions and derivations made in Ref. [33] are also summarized in Appendix A.

In this work the effective Lagrangian Eq. (1), is a scalar coupling that corresponds to the spin-coupling coefficients in which the Melosh rotations of the quark spin have the arguments defined by the kinematical momentum of the quarks in pair, and in the nucleon rest frame constrained by the total momentum [71, 72], while in the Bakamjian-Thomas construction the argument of the Melosh rotations are defined in the rest frame of three free particles (constituent quarks).

The model of the nucleon adopted here assumes the dominance of the valence component, and the pion (meson) cloud effects, which are known to be important to simultaneously describe well the proton and neutron EM form factors e.g., in the cloudy bag model [73], light-front treatment [74] and diquark approach [75], are not included explicitly. Within this approach, the results are strongly constrained, and the general features found in our calculations are rather independent of the detailed shape of the wave function, but depend on the momentum scales in Eq. (2). In the numerical evaluation of the form factors, we use a constituent quark mass value of $m_q = 0.22$ GeV [33, 58] as mentioned. This value was also used in the study of pion properties in vacuum as well as in medium [29–32] with a light-front constituent quark model. In addition, the model has three fitting parameters, the momentum scales β and β_1 , and the relative weight λ , or M_H (see Eqs. (2) and (3)). We have selected two parameter sets for the present two-scale model, which will be denoted by “set I” and “set II”, reproducing the proton magnetic moment (μ_p), and neutron magnetic moment (μ_n), respectively, as well as the zero of proton electric to magnetic form factor

ratio Q_0^2 for $\mu_p G_{Ep}(Q_0^2)/G_{Mp}(Q_0^2) = 0$, or $G_{Ep}(Q_0^2) = 0$. In Tab. I we summarize the model parameters for the set I and set II, some nucleon static observables calculated, and the zero, Q_0^2 , of $G_{Ep}(Q_0^2) = 0$.

TABLE I: Nucleon EM static observables and the zero of $G_{Ep}(Q_0^2) = 0$, Q_0^2 , for the two-scale models with the two sets of the parameters, set I and set II. The momentum-scale parameters, β, β_1 and M_H in Eqs. (2) and (3), are given in the second, third and fourth columns, respectively. The proton [neutron] magnetic moment μ_p [μ_n] (in nuclear magneton) and proton root-mean-square charge radius $r_p \equiv \langle r_p^2 \rangle^{1/2}$ [neutron mean-square charge radius r_n^2], are given in fifth [seventh] and sixth [eighth] columns respectively. The zero, Q_0^2 value for $G_{Ep}(Q_0^2) = 0$, is given in the last column. See Tab. II, for the experimental values.

	β (GeV)	β_1 (GeV)	M_H (GeV)	μ_p	r_p (fm)	μ_n	r_n^2 (fm) ²	Q_0^2 GeV ²
Set I	0.676	5.72	4.79	2.74	0.80	-1.52	-0.07	8.27
Set II	0.396	10.56	5.92	3.05	0.94	-1.88	-0.06	15.12

TABLE II: Experimental values for some nucleon observables.

Ref.	μ_p [μ_N]	$\sqrt{r_p^2}$ [fm]	μ_n [μ_N]	r_n^2 [fm ²]
[76, 77]	2.792847351 ± 10^{-9}	0.8751 ± 0.000061		
[78]		0.879 ± 0.0008		
[76]			-1.9130427 ± 5.10^{-7}	-0.1161 ± 0.0022

We remind that, a single-scale nucleon light-front wave function, Gaussian or power-law, with the proton or neutron magnetic moment fitted, is known to give a reasonable proton charge radius, due to the strong correlation between these observables [33, 54, 62]. However, the zero of $G_{Ep}(Q^2)$, Q_0^2 , appears at too small values in the range 3-4 GeV². When we attempt to fit Q_0^2 to the values around or larger than 8 GeV² by increasing the momentum scale in the Gaussian and power-law nucleon wave functions of the one-scale model, we find too small proton size, and consequently bad magnetic moment values. Thus, the facts leave us no room for improving the one-scale-based models. However, by introducing a two-scale,

namely, power-law high-momentum component in the wave function with the scalar coupling, we are able to get a reasonable description of both the nucleon static observables and the zero of $G_{Ep}(Q^2)$, as shown in Tab. I. The scalar coupling provides the best agreement with the neutron mean-square charge radius, when the neutron magnetic moment is fitted [33]. Note that, the high-momentum scale $M_H \sim 7.6$ GeV, should be understood as a reference value, and we point out that we cannot exclude completely the lower values for M_H , as one can see the parameterization, $M_H = 4.79$ GeV. Using these two parameter sets, set I and set II, we study the nucleon EM form factors in vacuum and in symmetric nuclear matter.

In Fig. 2 we show the results for the proton electric (upper panel) and magnetic (lower panel) form factors in vacuum, for the two sets of the parameters. The experimental data are well described by the set II.

Next, we show in Fig. 3 the form factor ratio, $\mu_p G_{Ep}(Q^2)/G_{Mp}(Q^2)$, calculated with the two parameter sets, the same as those in Fig. 2. Reasonable and better agreement with the data [37, 39–44] is achieved by the set II. The values of the zero for $G_{Ep}(Q^2)$, Q_0^2 , are given in Tab. I for both the set I and set II. The zero of the form factor ratio in vacuum by the set II, $Q_0^2 \simeq 15$ GeV², is one of the main results of this study. On the other hand, based on the nucleon Bethe-Salpeter amplitude and vector meson dominance model, Refs. [79, 80] report $Q_0^2 \simeq 9$ GeV². In addition, based on the covariant spectator quark model, Ref. [81] also obtained $Q_0^2 \simeq 9$ GeV² for $G_{Ep}(Q_0^2)/G_D(Q_0^2) = 0$, with $G_D(Q^2) = (1 + Q^2/0.71\text{GeV}^2)^{-2}$.

We show in Fig. 4, the neutron electric (upper panel) and magnetic (lower panel) form factors calculated in the two-scale model with the two sets of the parameters.

As one can see, the parameter set II describes better the data due to the strong sensitivity to $G_{En}(Q^2)$ [33]. Note that there is a zero in neutron magnetic form factor for the two-scale nucleon wave functions for the both parameter sets. The best fit for the experimental data of neutron magnetic form factor is achieved by the set II.

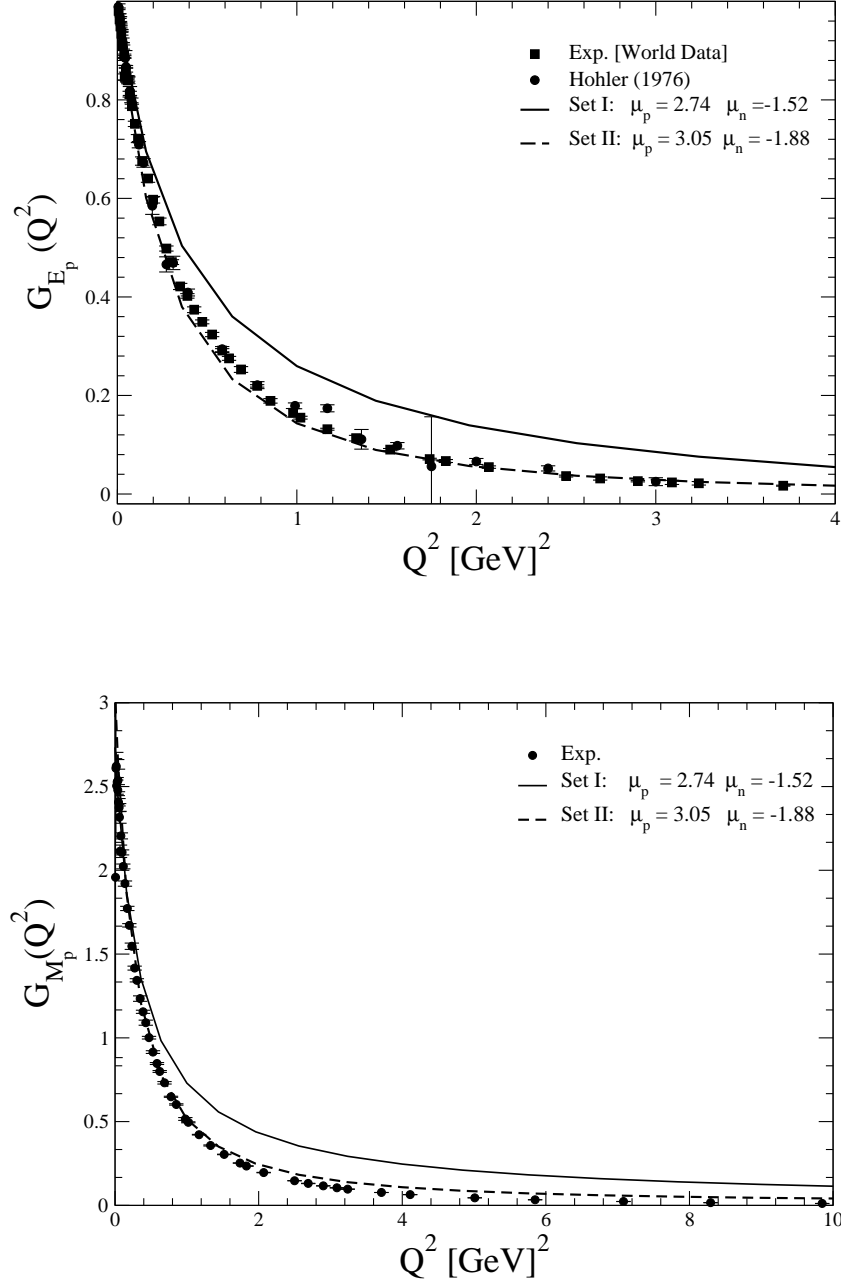


FIG. 2: Proton electric (upper panel) and magnetic (lower panel) form factors calculated by the two-scale model with the two parameter sets, set I (solid line), and set II (dashed line). (See also Tab. I.) Experimental data are from Refs. [37, 39–44, 82, 83].

III. QUARKS IN SYMMETRIC NUCLEAR MATTER: BRIEF REVIEW

In order to study the in-medium modifications of the nucleon EM form factors, we need a reasonable model of nuclear matter based on the quark degrees of freedom as well as the

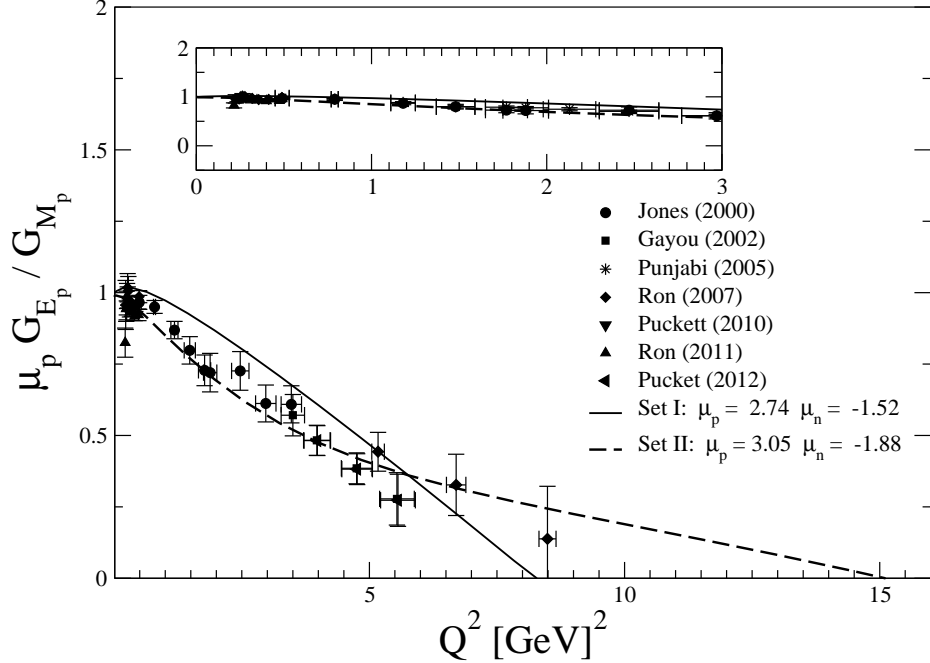


FIG. 3: Proton form factor ratio, $\mu_p G_{Ep}(Q^2)/G_{Mp}(Q^2)$, calculated by the two-scale model with the two parameter sets, set I and set II. Experimental data are from Refs. [37, 39–44].

nucleon model in vacuum, since our interest is the nucleon internal structure change in a nuclear medium.

As for the model of nuclear matter, we use the quark-meson coupling (QMC) model, which has been successfully applied for the studies of light-quark flavor as well as strange and charm hadron properties in a nuclear medium, and finite (hyper)nuclei [4, 84]. (The QMC model in early stage was also applied for finite nuclei in Ref. [85]. For more references on the “QMC” model from various other groups, readers are asked to consult Ref. [4].) This model was already used for the study of the in-medium pion properties [29–32] combined with a light-front constituent quark model. Therefore, we can extend the study of pion properties in medium for the in-medium nucleon EM form factors in a similar manner. We first review the quark model description of nuclear matter via the QMC model, and present the results for nuclear saturation properties as well as the in-medium constituent up and down quark properties, the same inputs used in the study of pion properties in medium [29–32].

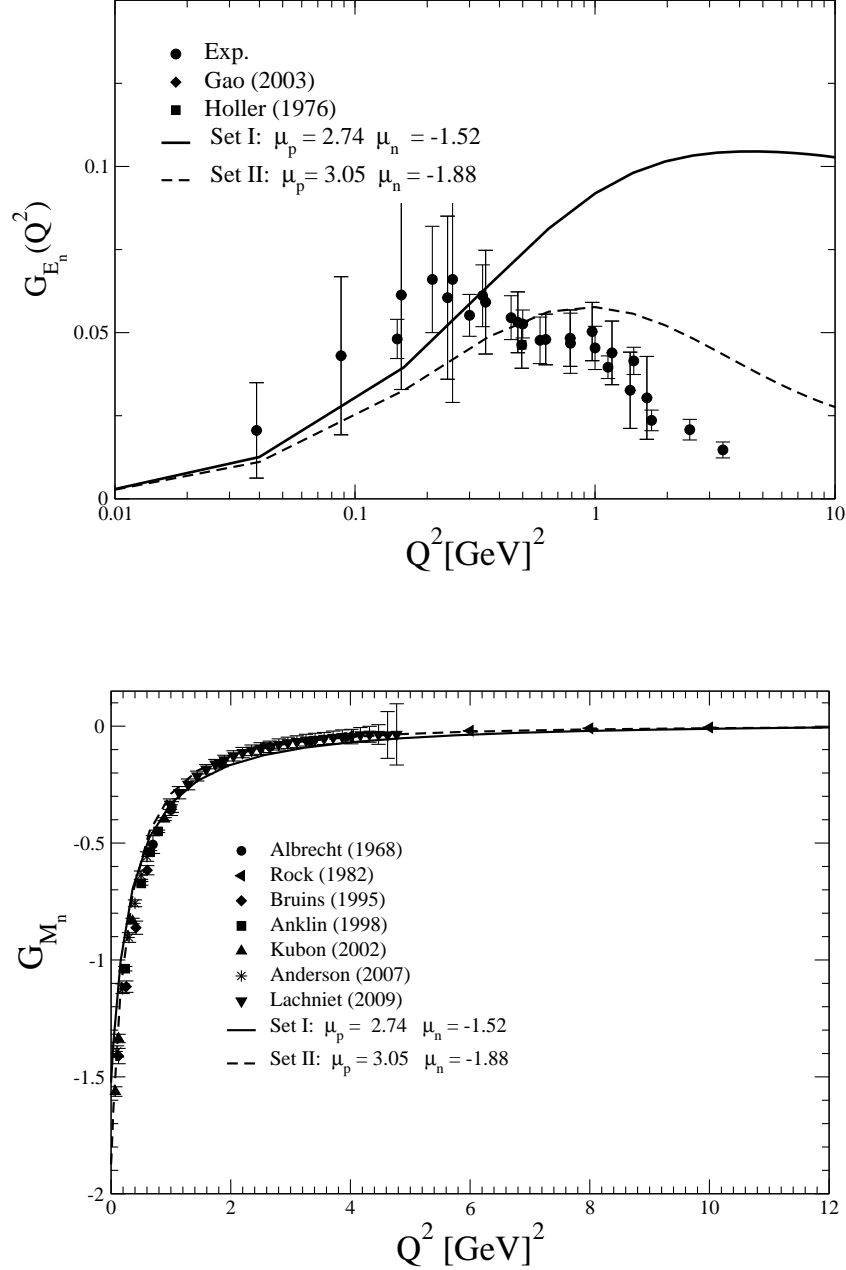


FIG. 4: Neutron electric (upper panel) and magnetic (lower panel) form factors calculated by the two-scale model with the two parameter sets. Experimental data are from [82, 83] for G_{E_n} , and from [88–94] for G_{M_n} .

A. Quark model of nuclear matter: quark-meson coupling (QMC) model

The QMC model was introduced by Guichon [3] in 1988 using the MIT bag model, and also by Frederico *et al.* in 1989 [23] using a confining harmonic potential, to describe the properties of nuclear matter based on the quark degrees of freedom. (See Ref. [4] for other

TABLE III: Coupling constants, the parameter Z_N , bag constant B (in $B^{1/4}$), and calculated properties for symmetric nuclear matter at normal nuclear matter density $\rho_0 = 0.15 \text{ fm}^{-3}$, for $m_q = 5$ and 220 MeV (the latter values is used in this study and Refs. [29–32]). The effective nucleon mass, m_N^* , and the nuclear incompressibility, K , are quoted in MeV (the free nucleon bag radius input is $R_N = 0.8 \text{ fm}$, the standard value in the QMC model [4]).

$m_q(\text{MeV})$	$g_\sigma^2/4\pi$	$g_\omega^2/4\pi$	m_N^*	K	Z_N	$B^{1/4}(\text{MeV})$
5	5.39	5.30	754.6	279.3	3.295	170
220	6.40	7.57	698.6	320.9	4.327	148

references.) In this study we use the model of Guichon with the MIT bag model. The model has been successfully applied for various studies of finite (hyper)nuclei [84] as well as the hadron properties in a nuclear medium [4]. In the model the medium effects arise from the self-consistent direct coupling of the isoscalar-Lorentz-scalar (σ), isoscalar-Lorentz-vector (ω) and isovector-Lorentz-vector (ρ) meson mean fields to the confined light-flavor u and d valence quarks — rather than to the nucleons. As a result the internal structure of the bound nucleon is modified by the surrounding nuclear medium with respect to the free nucleon.

The effective Lagrangian density of the QMC model for a uniform, spin-saturated, and isospin-symmetric infinite nuclear matter at the hadronic level is given by [3, 4, 84],

$$\mathcal{L} = \bar{\psi}[i\gamma \cdot \partial - m_N^*(\hat{\sigma}) - g_\omega \hat{\omega}^\mu \gamma_\mu]\psi + \mathcal{L}_{\text{meson}}, \quad (8)$$

where ψ , $\hat{\sigma}$ and $\hat{\omega}$ are respectively the nucleon, Lorentz-scalar-isoscalar σ , and Lorentz-vector-isoscalar ω field operators, with

$$m_N^*(\hat{\sigma}) \equiv m_N - g_\sigma(\hat{\sigma})\hat{\sigma}, \quad (9)$$

which defines the σ -field dependent coupling constant, $g_\sigma(\hat{\sigma})$, while g_ω is the nucleon- ω coupling constant. All the important effective nuclear many-body dynamics including 3-body nucleon force modeled at the quark level, can be regarded as effectively condensed in $g_\sigma(\hat{\sigma})$. Solving the Dirac equations for the up and down quarks in the nuclear medium with the same mean fields (mean values) σ and ω which act on the bound nucleon self-consistently based on Eq. (8), we obtain the effective σ -dependent coupling $g_\sigma(\sigma)$ at the

nucleon level [3, 4, 84]. The free meson Lagrangian density is given by,

$$\mathcal{L}_{\text{meson}} = \frac{1}{2}(\partial_\mu \hat{\sigma} \partial^\mu \hat{\sigma} - m_\sigma^2 \hat{\sigma}^2) - \frac{1}{2} \partial_\mu \hat{\omega}_\nu (\partial^\mu \hat{\omega}^\nu - \partial^\nu \hat{\omega}^\mu) + \frac{1}{2} m_\omega^2 \hat{\omega}^\mu \hat{\omega}_\mu, \quad (10)$$

where we have ignored the isospin-dependent Lorentz-vector-isovector ρ -meson field, since we consider isospin-symmetric nuclear matter within the Hartree mean-field approximation. In this case the mean value of the ρ -meson field becomes zero and there is no need to consider its possible contributions due to the ρ -Fock (exchange) terms.

In the following we work in the nuclear matter rest frame. For symmetric nuclear matter in the Hartree mean-field approximation, the nucleon Fermi momentum k_F (baryon density ρ) and the scalar density (ρ_s) associated with the σ -mean field can be related as,

$$\rho = \frac{4}{(2\pi)^3} \int d^3k \theta(k_F - |\vec{k}|) = \frac{2k_F^3}{3\pi^2}, \quad (11)$$

$$\rho_s = \frac{4}{(2\pi)^3} \int d^3k \theta(k_F - |\vec{k}|) \frac{m_N^*(\sigma)}{\sqrt{m_N^{*2}(\sigma) + \vec{k}^2}}, \quad (12)$$

where $m_N^*(\sigma)$ is the constant value of the effective nucleon mass at a given density, and is calculated in the standard QMC model [3, 4, 84]. The Dirac equations for the up (u) and down (d) quarks in symmetric nuclear matter are solved self-consistently with the same σ and ω mean-field potentials acting for the nucleon. We restrict ourselves hereafter the flavor SU(2), the u and d quark sector (as well as for the proton and neutron). The Dirac equations for the quarks and antiquarks ($q = u$ or d , quarks) in the bag of hadron h in nuclear matter at the position $x = (t, \vec{r})$ ($|\vec{r}| \leq$ bag radius) are given by [4],

$$\left[i\gamma \cdot \partial_x - (m_q - V_\sigma^q) \mp \gamma^0 \left(V_\omega^q + \frac{1}{2} V_\rho^q \right) \right] \begin{pmatrix} \psi_u(x) \\ \psi_{\bar{u}}(x) \end{pmatrix} = 0, \quad (13)$$

$$\left[i\gamma \cdot \partial_x - (m_q - V_\sigma^q) \mp \gamma^0 \left(V_\omega^q - \frac{1}{2} V_\rho^q \right) \right] \begin{pmatrix} \psi_d(x) \\ \psi_{\bar{d}}(x) \end{pmatrix} = 0, \quad (14)$$

where we have neglected the Coulomb force as usual, since the nuclear matter properties are due to the strong interaction, and we assume SU(2) symmetry for the light-flavor u and s quarks, $m_q = m_u = m_d$, and define $m_q^* \equiv m_q - V_\sigma^q = m_u^* = m_d^*$. In symmetric nuclear matter, the isospin dependent ρ -meson mean field in Hartree approximation yields $V_\rho^q = 0$ in Eqs. (13) and (14), as mentioned already, so we ignore it hereafter. The constant mean-field potentials in (symmetric) nuclear matter are defined by, $V_\sigma^q \equiv g_\sigma^q \sigma = g_\sigma^q \langle \sigma \rangle$

and $V_\omega^q \equiv g_\omega^q \omega = g_\omega^q \delta^{\mu,0} \langle \omega^\mu \rangle$, with g_σ^q and g_ω^q being the corresponding quark-meson coupling constants, and the quantities inside the brackets stand for taking expectation values by the nuclear matter ground state [4]. Note that, since the velocity averages to zero in the rest frame of nuclear matter, the mean vector source due to the quark fields as well, $\langle \bar{\psi}_q \vec{\gamma} \psi_q \rangle = 0$. Thus we may just keep the term proportional to γ^0 in Eqs. (13) and (14).

The normalized, static solution for the ground state quarks or antiquarks with flavor f in the hadron h composed of u and d quarks, may be written, $\psi_f(x) = N_f e^{-i\epsilon_f t/R_h^*} \psi_f(\vec{r})$, where N_f and $\psi_f(\vec{r})$ are the normalization factor and corresponding spin and spatial part of the wave function. The bag radius in medium for a hadron h , R_h^* , is determined through the stability condition for the mass of the hadron against the variation of the bag radius [4]. The eigenenergies in units of $1/R_h^*$ are given by,

$$\begin{pmatrix} \epsilon_u \\ \epsilon_{\bar{u}} \end{pmatrix} = \Omega_q^* \pm R_h^* \left(V_\omega^q + \frac{1}{2} V_\rho^q \right), \quad \begin{pmatrix} \epsilon_d \\ \epsilon_{\bar{d}} \end{pmatrix} = \Omega_q^* \pm R_h^* \left(V_\omega^q - \frac{1}{2} V_\rho^q \right). \quad (15)$$

The hadron masses in a nuclear medium m_h^* (free mass m_h), are calculated by

$$m_h^* = \sum_{j=q,\bar{q}} \frac{n_j \Omega_j^* - z_h}{R_h^*} + \frac{4}{3} \pi R_h^{*3} B, \quad \left. \frac{\partial m_h^*}{\partial R_h^*} \right|_{R_h=R_h^*} = 0, \quad (16)$$

where $\Omega_q^* = \Omega_{\bar{q}}^* = [x_q^2 + (R_h^* m_q^*)^2]^{1/2}$, with $m_q^* = m_q - g_\sigma^q \sigma$, and x_q being the lowest bag eigenfrequencies. $n_q(n_{\bar{q}})$ is the quark (antiquark) numbers for the quark flavors q . The MIT bag quantities, z_h , B , x_q , and m_q are the parameters for the sum of the c.m. and gluon fluctuation effects, bag constant, lowest eigenvalues for the quarks q , and the corresponding current quark masses. z_N and B (z_h) are fixed by fitting the nucleon (the hadron) mass in free space. (See Tab. III for the nucleon case.)

For the nucleon $h = N$ in the above, the lowest, positive energy bag eigenfunction is given by

$$q(t, \vec{r}) = \frac{\mathcal{N}}{\sqrt{4\pi}} e^{-i\epsilon_q t/R_N^*} \begin{pmatrix} j_0(xr/R_N^*) \\ i\beta_q \vec{\sigma} \cdot \hat{r} j_1(xr/R_N^*) \end{pmatrix} \theta(R_N^* - r) \chi_m, \quad (17)$$

with $r = |\vec{r}|$ and χ_m the spin function and

$$\Omega_q^* = \sqrt{x^2 + (m_q^* R_N^*)^2}, \quad \beta_q = \sqrt{\frac{\Omega_q^* - m_q^* R_N^*}{\Omega_q^* + m_q^* R_N^*}}, \quad (18)$$

$$\mathcal{N}^{-2} = 2R_N^{*3} j_0^2(x) [\Omega_q^* (\Omega_q^* - 1) + m_q^* R_N^* / 2] / x^2, \quad (19)$$

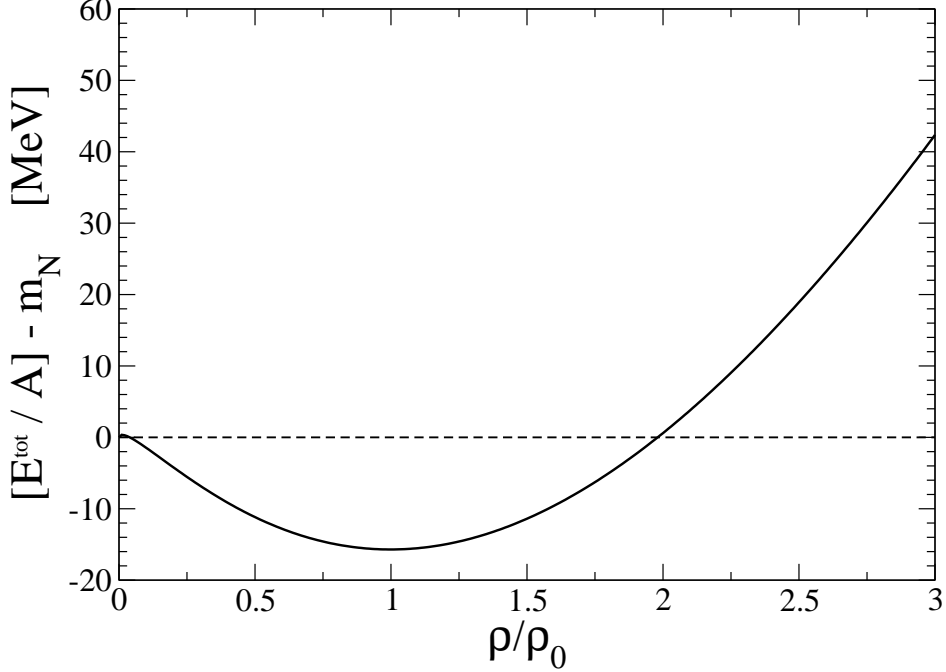


FIG. 5: Negative of the binding energy per nucleon ($E^{\text{tot}}/A - m_N$) for symmetric nuclear matter calculated with the vacuum up and down quark mass, $m_q = 220$ MeV, taken from Ref. [29–32]. At the saturation point $\rho_0 = 0.15 \text{ fm}^{-3}$, the value is fitted to -15.7 MeV. (See Ref. [4] for the $m_q = 5$ MeV case, denoted in there as QMC-I.)

where x is the eigenvalue for the lowest mode, which satisfies the boundary condition at the bag surface, $j_0(x) = \beta_q j_1(x)$ with $j_{0,1}$ are the spherical Bessel functions.

The same meson mean fields σ and ω for the quarks and nucleons satisfy the following equations at the nucleon level self-consistently:

$$\omega = \frac{g_\omega \rho}{m_\omega^2}, \quad (20)$$

$$\sigma = \frac{g_\sigma}{m_\sigma^2} C_N(\sigma) \frac{4}{(2\pi)^3} \int d^3k \theta(k_F - |\vec{k}|) \frac{m_N^*(\sigma)}{\sqrt{m_N^{*2}(\sigma) + \vec{k}^2}} = \frac{g_\sigma}{m_\sigma^2} C_N(\sigma) \rho_s, \quad (21)$$

$$C_N(\sigma) = \frac{-1}{g_\sigma(\sigma=0)} \left[\frac{\partial m_N^*(\sigma)}{\partial \sigma} \right], \quad (22)$$

where $C_N(\sigma)$ is the constant value of the scalar density ratio [3, 4, 84]. Because of the underlying quark structure of the nucleon used to calculate $M_N^*(\sigma)$ in the nuclear medium (see Eq. (16) with $h = N$), $C_N(\sigma)$ gets nonlinear σ -dependence, whereas the usual point-like nucleon-based model yields unity, $C_N(\sigma) = 1$. It is this $C_N(\sigma)$ or $g_\sigma(\sigma)$ that gives

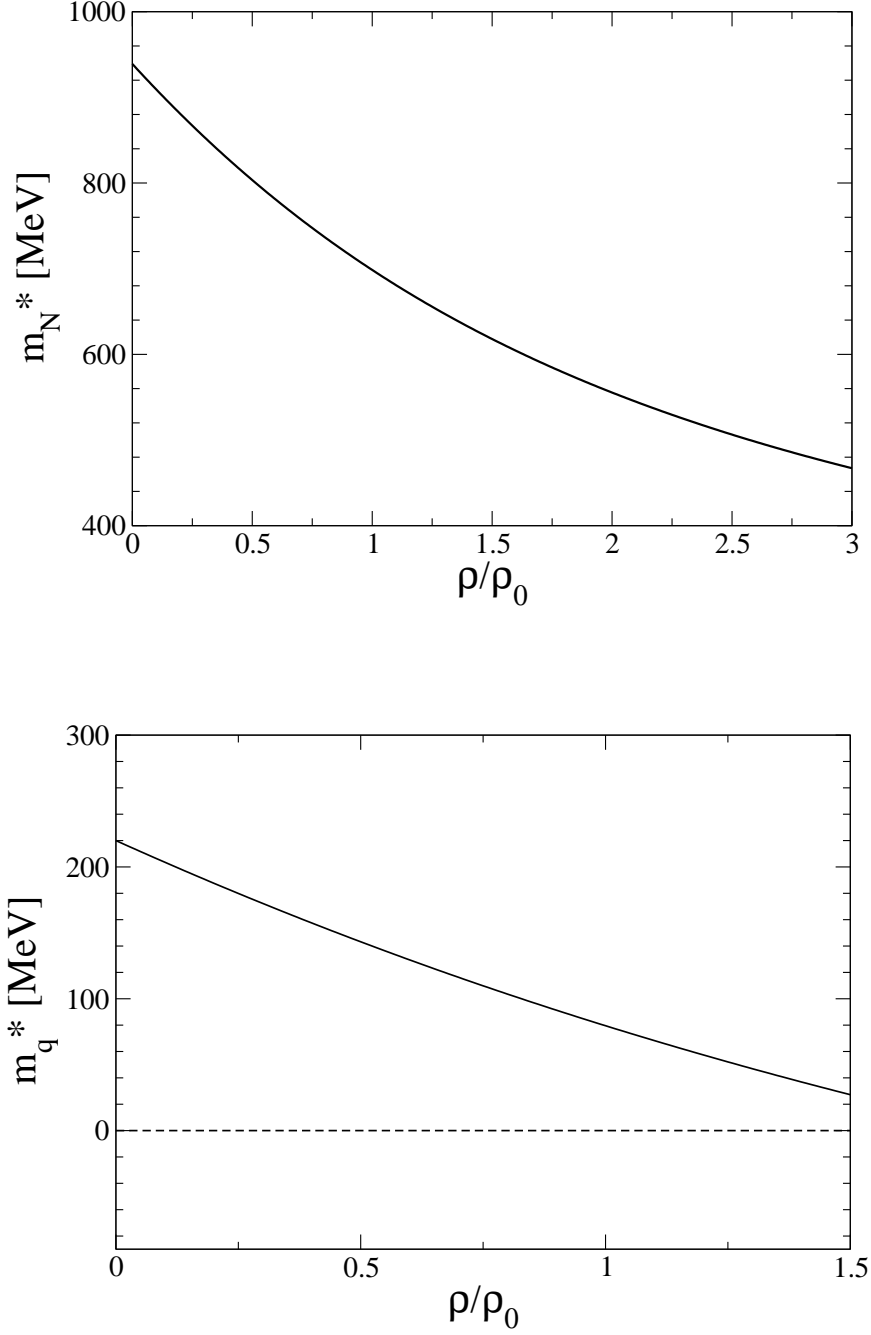


FIG. 6: Nucleon and constituent quark effective masses, respectively m_N^* (upper panel), and m_q^* (lower panel) where $m_q^* \equiv m_u^* = m_d^*$, in symmetric nuclear matter taken from Refs. [29–32]. See also caption of Fig. 5.

a novel saturation mechanism in the QMC model, and contains the important dynamics which originates from the quark structure of the nucleon. Without an explicit introduction of the nonlinear couplings of the meson fields in the Lagrangian density at the nucleon and meson level, the standard QMC model yields the nuclear incompressibility of $K \simeq 280$ MeV with $m_q = 5$ MeV, which is in contrast to a naive version of quantum hadrodynamics (QHD) [95] (the point-like nucleon model of nuclear matter), results in the much larger value, $K \simeq 500$ MeV; the empirically extracted value falls in the range $K = 200 - 300$ MeV. (See Ref. [96] for the updated discussions on the incompressibility.)

Once the self-consistency equation for the σ , Eq. (21), has been solved, one can evaluate the total energy per nucleon:

$$E^{\text{tot}}/A = \frac{4}{(2\pi)^3 \rho} \int d^3k \theta(k_F - |\vec{k}|) \sqrt{m_N^*(\sigma) + \vec{k}^2} + \frac{m_\sigma^2 \sigma^2}{2\rho} + \frac{g_\omega^2 \rho}{2m_\omega^2}. \quad (23)$$

We then determine the coupling constants, g_σ and g_ω , so as to fit the binding energy of 15.7 MeV at the saturation density $\rho_0 = 0.15 \text{ fm}^{-3}$ ($k_F^0 = 1.305 \text{ fm}^{-1}$) for symmetric nuclear matter.

In the study of pion properties in medium [29–32] based on a light-front constituent quark model, the vacuum value of the u and d quark constituent mass, $m_q = 220$ MeV was used and could reproduce well the EM form factor and decay constant in vacuum [45].

To be consistent and encouraged by the studies for the pion properties in a nuclear medium [29–32], we build the nuclear matter with the same u and d constituent quark mass in vacuum. The corresponding coupling constants and some results for symmetric nuclear matter at the saturation density calculated with $m_q = 220$ MeV and the standard values of $m_\sigma = 550$ MeV and $m_\omega = 783$ MeV, are listed in Tab. III. For comparison, we also give the corresponding quantities calculated in the standard QMC model with a vacuum quark mass of $m_q = 5$ MeV (see Ref. [4] for details). Thus, we have obtained the in-medium properties of the u and d constituent quarks in symmetric nuclear matter with the vacuum mass of $m_q = 220$ MeV. Namely, we obtain the density dependence of the effective mass (scalar potential) and vector potential. Using the obtained in-medium inputs, we study the nucleon EM form factors in symmetric nuclear matter.

In Figs. 5 and 6, we respectively show the results for the negative of the binding energy per nucleon ($E^{\text{tot}}/A - m_N$), effective mass of the nucleon, m_N^* , and effective mass of the constituent up and down quarks, m_q^* , in symmetric nuclear matter.

As one can expect from the values of the incompressibility, $K = (279.3, 320.9)$ MeV for m_q (5, 220) MeV, in Tab. III, the result for $E/A - m_N$ with $m_q = 220$ MeV shown in Fig. 5 varies slightly faster than that for the case of $m_q = 5$ MeV [4] as increasing nuclear matter density. As for the effective nucleon mass shown in Fig. 6 with $m_q = 220$ MeV, it also decreases faster than that for $m_q = 5$ MeV [4] as increasing nuclear matter density.

In next section we study the nucleon EM form factors in a nuclear medium using the in-medium constituent quark properties obtained so far.

IV. NUCLEON ELECTROMAGNETIC FORM FACTORS IN MEDIUM

In this section we present our main results, the nucleon EM form factors in symmetric nuclear matter, $G_{Ep}^*(Q^2)$, $G_{Mp}^*(Q^2)$, $G_{En}^*(Q^2)$, $G_{Mn}^*(Q^2)$, the ratio, $\mu_p G_{Ep}^*(Q^2)/G_{Mp}^*(Q^2)$, and the double ratio, $R_p \equiv [G_{Ep}^*(Q^2)/G_{Mp}^*(Q^2)]/[G_{Ep}(Q^2)/G_{Mp}(Q^2)]$, and the corresponding double ratio for neutron, R_n . Our interests in this section are, in-medium effects on the zero of $\mu_p G_{Ep}^*(Q^2)/G_{Mp}^*(Q^2)$, and the comparison with the JLab data for $[G_{Ep}^{4\text{He}}(Q^2)/G_{Mp}^{4\text{He}}(Q^2)]/[G_{Ep}^{1\text{H}}(Q^2)/G_{Mp}^{1\text{H}}(Q^2)]$, as well as the corresponding neutron EM form factor double ratio R_n in symmetric nuclear matter.

Before presenting the results for the in-medium nucleon EM form factors, we briefly explain how the nucleon is treated in medium within the present model. The description of the nucleon in vacuum, and the calculation of the relevant microscopic EM matrix elements are explained in Appendix A. The starting point is the relativistic invariant effective Lagrangian density in vacuum Eq. (1). Then the calculation in vacuum is made by the light-front projection with the *relativistic quark-spin coupling model*, a light-front constituent quark model. Although it would be idealistic to construct the nuclear matter also within the same model with the nucleon substructure, it would be a very difficult task to achieve properly with being guaranteed by phenomenological success. In particular, this is true when we try to describe the nuclear matter based on the quark degrees of freedom within the same model. In fact, light-front based nuclear mean field theory [86] and some applications exist [87], but we would like to take a practical manner to adapt the in-medium inputs necessary from the quark-based successful model, the QMC model [4, 84], which has already been explained in Sec. III.

What characterize the in-medium properties of nucleon and u and d quarks in medium

are, the Lorentz-scalar and Lorentz-vector mean field potentials felt by the nucleon and the u and d quarks in medium, consistently obtained with the nuclear matter saturation properties. For this purpose, we rely on the quark-based successful model, the QMC model. Then, based on the explanations given in Appendix A, the in-medium treatment is made as follows. The momentum of the light quark j ($j = 1, 2, 3$) in the nucleon, k_j^μ , is replaced by $k_j^{*\mu} = (k_j^0 + V_\omega^q, \vec{k}_j)$, where V_ω^q is the vector mean field potential felt by a light-flavor quark in symmetric nuclear matter. (Space component of the momentum is not modified in the present case of Hartree mean field approximation.) Correspondingly, the in-medium light-front momentum is defined by $k_j^{*+} = k_j^{*0} + k_j^3$. Since the nucleon consists of three light quarks, its momentum in free space p^μ is replaced by $p^{*\mu} = (p^0 + 3V_\omega^q, \vec{p}) = (\sqrt{m_N^{*2} + \vec{p}^2} + 3V_\omega^q, \vec{p})$, and thus the corresponding in-medium light-front plus-momentum becomes $p^{*+} = p^{*0} + p^3 = (\sqrt{m_N^{*2} + \vec{p}^2} + 3V_\omega^q) + p^3$. Furthermore, the quark and nucleon masses in vacuum m_q and m_N are respectively replaced by $m_q \rightarrow m_q^*$ and $m_N \rightarrow m_N^*$, whenever they appear in the expressions in vacuum. Note that, for the Dirac particle spinor in medium with its three-momentum \vec{k} , the energy $E_N^*(\vec{k}) = \sqrt{m_N^{*2} + \vec{k}^2}$ is used without the vector potential $3V_\omega^q$ [97]. These in-medium inputs m_q^* , V_ω^q and m_N^* , are calculated by the QMC model for a given nuclear matter density as explained above. (See also Sec. III.)

In the following we present results for the in-medium nucleon EM form factors. We note that the nuclear matter densities $\rho = 0.3\rho_0$ and $0.4\rho_0$ studied in this section (except for the set II in Fig. 10), are chosen so that to give a trend of medium effects, based on a rough estimate made for the proton EM double ratio by the set I to be shown later in Fig. 10. First, we give in Tab. IV some static properties of nucleon in medium together with those in vacuum.

One can notice that the magnetic moments of proton and neutron in medium are enhanced as nuclear matter density increases for the both parameters sets I and II. So do the in-medium proton root-mean-square charge radius r_p^* and neutron mean-square charge radius r_n^{*2} . These features are in agreement with those found in Ref. [98] studied in the QMC model. One of the very interesting quantities is Q_0^{2*} , the value of crossing zero, namely the value satisfying $G_{Ep}^*(Q_0^{2*}) = 0$. The values of Q_0^{2*} decrease as nuclear matter density increases for the both parameter sets I and II. The corresponding figure will be shown in Fig. 8.

Next, we show in Fig. 7 in-medium proton electric $G_{Ep}^*(Q^2)$ (upper panel) and magnetic G_{Mp}^* (lower panel) form factors in the two-scale model with the two parameter sets, set I

TABLE IV: Nucleon EM static observables and the zero of $G_{Ep}(Q_0^{2*}) = 0$, Q_0^{2*} , for the two-scale models with the two sets of the parameters, set I and set II for densities $\rho/\rho_0 = 0.0, 0.3$ and 0.4 . (See also caption of Tab. I.)

	ρ/ρ_0	μ_p^*	r_p^* (fm)	μ_n^*	r_n^{2*} (fm) ²	Q_0^{2*} GeV ²
Set I	0.0	2.74	0.80	-1.52	-0.07	8.27
	0.3	2.91	0.95	-1.68	-0.13	7.12
	0.4	2.96	1.00	-1.72	-0.15	6.78
Set II	0.0	3.05	0.94	-1.88	-0.06	15.12
	0.3	3.23	1.08	-2.05	-0.11	6.34
	0.4	3.29	1.18	-2.11	-0.12	5.10

and set II, for nuclear matter densities of $\rho = 0.3\rho_0$ and $0.4\rho_0$ ($\rho_0 = 0.15 \text{ fm}^{-3}$), together with those in vacuum to make easier to see the medium effects. For $G_{Ep}^*(Q^2)$, the falloff becomes faster as increasing nuclear matter density than that in vacuum. This means that the proton mean-square charge radius increases in symmetric nuclear matter. The fast falloff of the electric form factor was also found in Refs. [98, 99]. From this behavior, we can expect that the zero of $G_{Ep}^*(Q^2)$ in medium shifts to a smaller Q^2 value.

As for $G_{Mp}^*(Q^2)$, the in-medium proton magnetic moment $\mu_p^* = G_{Mp}^*(0)$ is enhanced than that in vacuum as increasing nuclear matter density. This enhancement is also, observed in Refs. [98, 99]. However, as increasing Q^2 , the falloff of the in medium one, $G_{Mp}^*(Q^2)$, becomes faster than that in vacuum.

To understand better the in-medium effect on the nucleon EM form factors, we show the results without the vector potential, namely, the results only included the effects of the nucleon and quark mass shifts in medium for $G_{Ep}^*(Q^2)$ (upper panel) and $G_{Mp}^*(Q^2)$ (lower panel). They are denoted by “w/o VP” in Fig. 7 for $\rho/\rho_0 = 0.3$ and 0.4 . One can see that the effect of the vector potential is very small for both parameter sets I and II. Typically the effect is a few percent at most for the corresponding density, and cannot be distinguished well from the full result with the vector potential. This feature is also reflected from the densities treated here are relatively small, and thus the effect of the vector potential becomes small. Nevertheless, we can see the effect of the mass shifts is larger than that of the vector

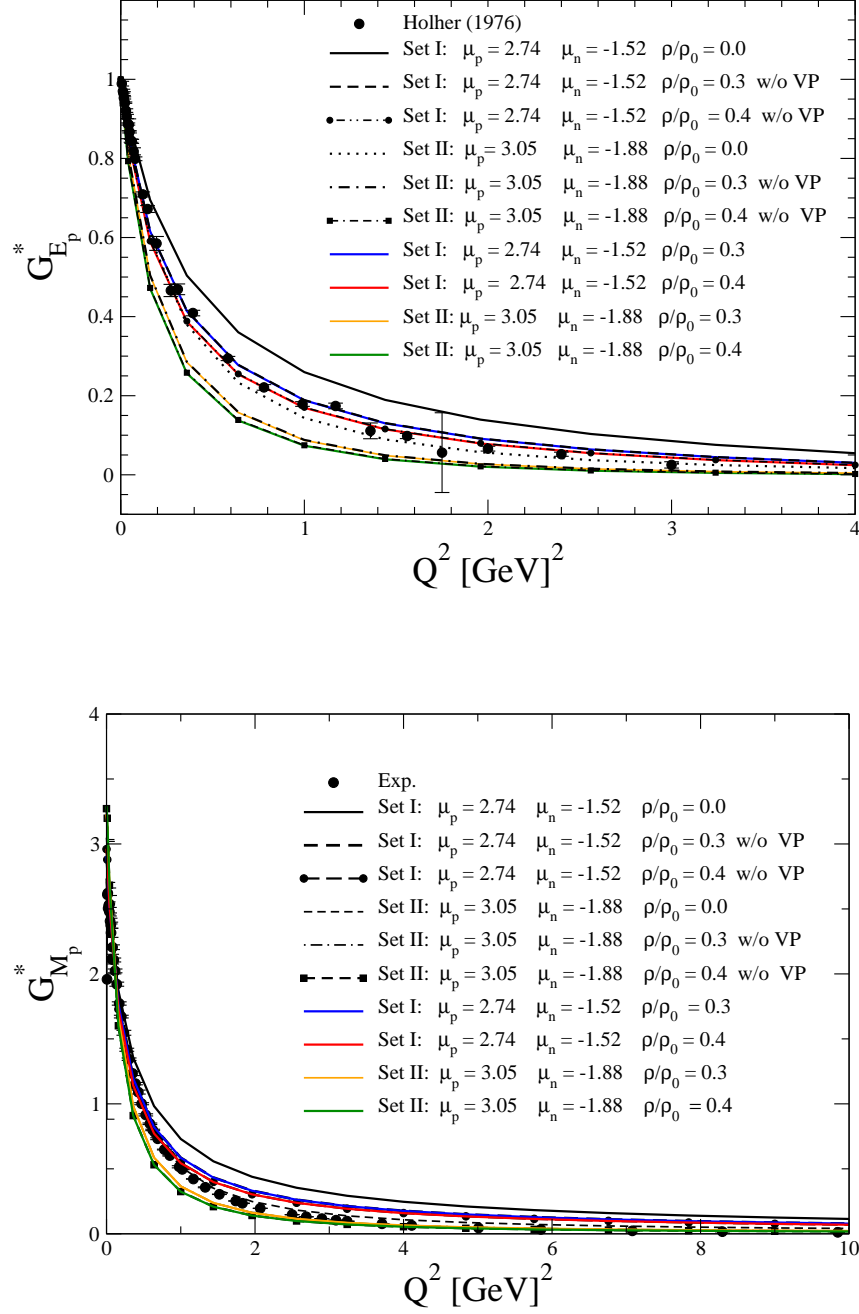


FIG. 7: Proton electric $G_{Ep}^*(Q^2)$ (upper panel), and magnetic form $G_{Mp}^*(Q^2)$ (lower panel) form factors calculated in the two-scale model with the two parameter sets, set I and set II, for nuclear matter densities $\rho = 0.3\rho_0$ and $0.4\rho_0$ with $\rho_0 = 0.15 \text{ fm}^{-3}$, together with those in vacuum. (See also Tab. I.) In figure, “w/o VP” stands for the result calculated without the vector potential. Experimental world data are from [100–106].

potential in the present model. We have also studied the effect of the vector potential for all the other EM form factors, and confirmed that the effect is small. Thus, we will not show the other EM form factor results calculated without the vector potential.

Based on the results shown in Fig. 7, we show in Fig. 8 the result for $\mu_p^* G_{Ep}^*(Q^2)/G_{Mp}^*(Q^2)$, in symmetric nuclear matter as well as in vacuum.

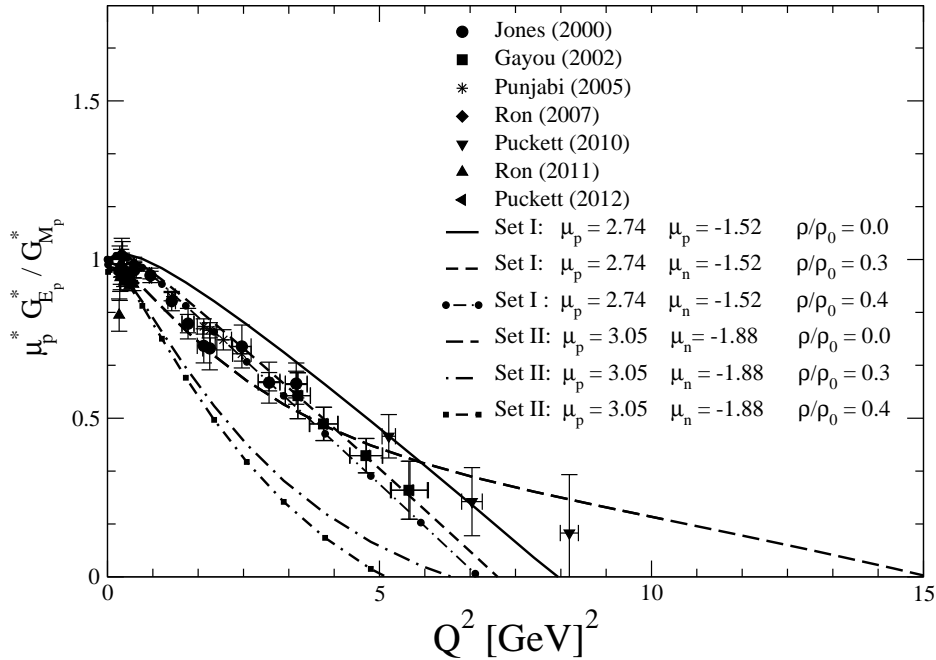


FIG. 8: $\mu_p^* G_{Ep}^*(Q^2)/G_{Mp}^*(Q^2)$ calculated by the two-scale model with the two parameter sets, for the nuclear matter densities $\rho = 0.3\rho_0$ and $0.4\rho_0$.

This is our second main results and prediction of this article. For each parameter set, the value of Q_0^{2*} to cross zero satisfying $\mu_p^* G_{Ep}^*(Q_0^{2*})/G_{Mp}^*(Q_0^{2*}) = 0$, becomes smaller than that in vacuum. This reflects that the in-medium falloff of $G_{Ep}^*(Q^2)$ becomes faster than that in vacuum as already mentioned. Thus, it is very interesting to pursue experiment to measure the proton EM form factor ratio of the bound proton, to check if this Q^2 reduction of crossing the zero can be observed, although such experiment would be very challenging. However, we would like to emphasize that this is a very interesting prediction of the present study. We believe that this is the first time prediction which is made with an explicit calculation.

Next, in Fig. 9 we show the in-medium neutron electric $G_{En}^*(Q^2)$ (upper panel), and magnetic $G_{Mn}^*(Q^2)$ (lower panel) form factors.

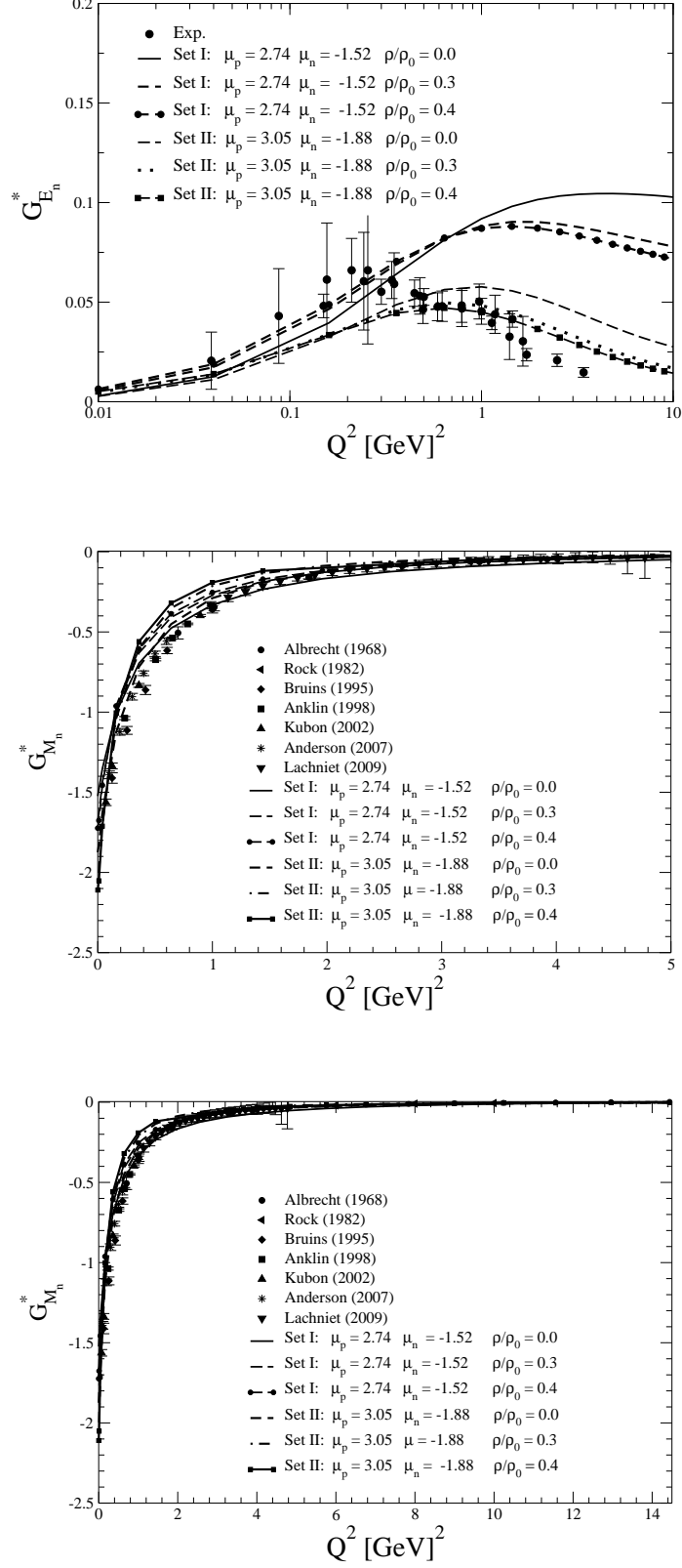


FIG. 9: Neutron electric $G_{En}^*(Q^2)$ (upper panel) and magnetic $G_{Mn}^*(Q^2)$ (middle and bottom panels) form factors in medium, obtained by the two-scale model with the two sets of parameters, for $\rho = 0.3\rho_0$ and $0.4\rho_0$. Those in vacuum are shown for references.

For both parameter sets, set I and set II, $G_{E_n}^*(Q^2)$ is suppressed than that in vacuum as increasing Q^2 , while very small region of Q^2 , $G_{E_n}^*(Q^2)$ is enhanced than that in vacuum.

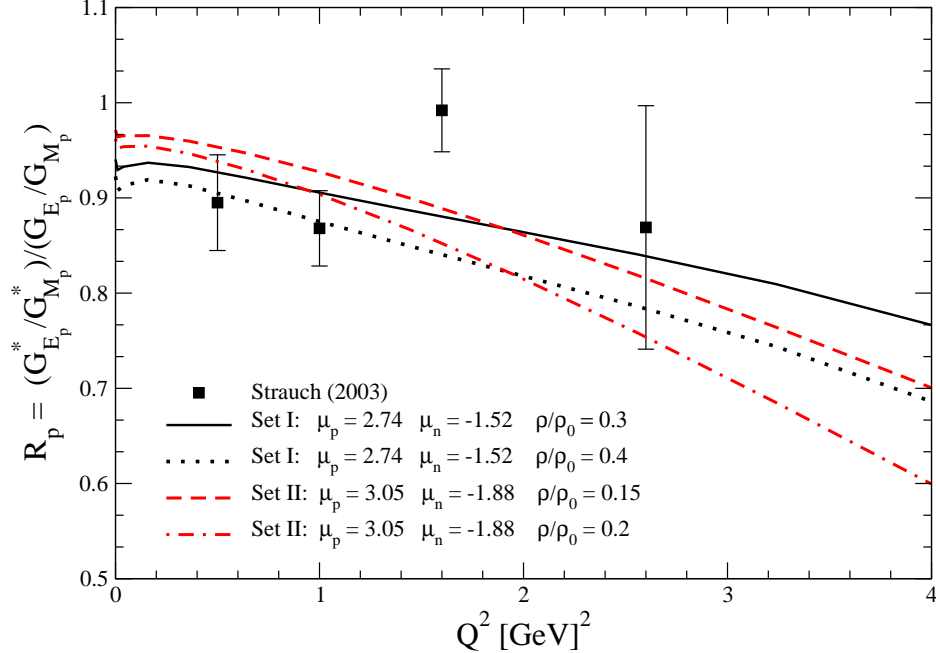


FIG. 10: Proton EM form factor double ratio in symmetric nuclear matter, $R_p \equiv [G_{E_p}^*(Q^2)/G_{M_p}^*(Q^2)]/[G_{E_p}(Q^2)/G_{M_p}(Q^2)]$, calculated by the two-scale model with the two parameter sets, with the set I for nuclear matter densities $0.30\rho_0$ and $0.40\rho_0$, and with the set II for nuclear matter densities $0.15\rho_0$ and $0.20\rho_0$, compared with the JLab data extracted for $[G_{E_p}^{4\text{He}}(Q^2)/G_{M_p}^{4\text{He}}(Q^2)]/[G_{E_p}^{1\text{H}}(Q^2)/G_{M_p}^{1\text{H}}(Q^2)]$. The experimental data are taken from Ref. [17].

As for the magnetic form factor, the absolute values in medium $|G_{M_n}^*(Q^2)|$, becomes smaller than that in vacuum for whole region of Q^2 studied. This means that the “negative falloff” becomes faster, or Q^2 dependence becomes more sensitive, similar trend as that found for the proton.

In Fig. 10, we show our third main result of this article, the result of the proton form factor double ratio, $[G_{E_p}^*(Q^2)/G_{M_p}^*(Q^2)]/[G_{E_p}(Q^2)/G_{M_p}(Q^2)]$ in symmetric nuclear matter, by the two-scale model with the set I and set II, compared with the JLab data. The good description of the JLab data is obtained by the both parameter sets, set I and set II, by adjusting different nuclear matter densities. Namely, for the set I with the nuclear matter density $0.3\rho_0$, and for the set II the nuclear matter density $0.15\rho_0$, the JLab data are well

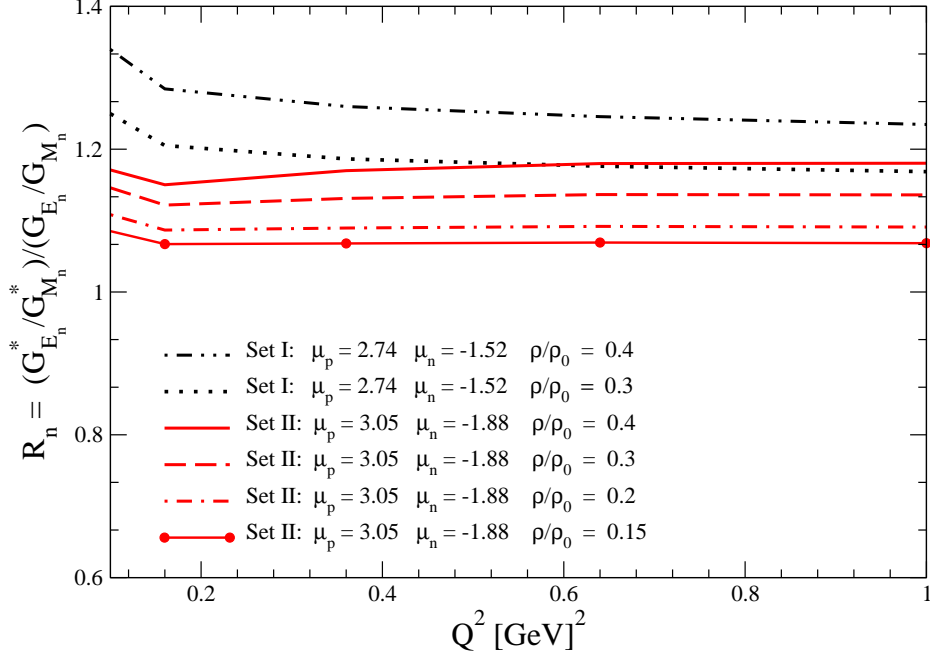


FIG. 11: Neutron EM form factor double ratio in symmetric nuclear matter, $R_n \equiv [G_{En}^*(Q^2)/G_{Mn}^*(Q^2)]/[G_{En}(Q^2)/G_{Mn}(Q^2)]$, calculated by the two-scale model with the two parameter sets, with the set I and set II for nuclear matter densities $0.30\rho_0$ and $0.40\rho_0$, and with the set II for nuclear matter densities $0.15\rho_0$ and $0.20\rho_0$. The results are shown for the Q^2 range, $0.1 < Q^2 < 1 \text{ GeV}^2$. (See also caption of Fig. 10.)

described. Recall that the zero of $\mu_p G_{Ep}(Q^2)/G_{Mp}(Q^2)$ and the nucleon EM form factors in vacuum can be better described with the set II.

We have also calculated the double ratio using the one-scale model that fits experimental proton magnetic moment better for the nuclear matter densities $0.3\rho_0$ and $0.4\rho_0$ as examples. But it gives a very poor description of the data, and thus we do not show the results. For a comparison between the one-scale and two-scale models made in the past, see Ref. [72].

Finally, similar to the proton EM form factor double ratio, we also show the calculated, corresponding very interesting double ratio for the neutron in symmetric nuclear matter R_n , where this quantity is predicted in Ref. [28] to be enhanced in medium relative to that in vacuum for small Q^2 range ($0.1 < Q^2 < 1 \text{ GeV}^2$), while that for the proton in medium is quenched. We show in Fig. 11 the calculated double ratios for the nuclear matter densities $\rho = 0.3\rho_0$ and $0.4\rho_0$ for the two parameter sets, as well as $\rho = 0.15\rho_0$ and $0.20\rho_0$ for the set II. The results show that the enhancement of the ratio in nuclear matter relative to

that in vacuum. (Note that proton case for the densities $0.3\rho_0$ and $0.4\rho_0$ are quenched, although all the results are not shown explicitly except for the results shown in Fig. 10.) Thus, our results agree with the prediction made in Ref. [28]. Note that, all the double ratio R_n calculated in symmetric nuclear matter with the densities chosen in this study, is enhanced and larger than unity for the Q^2 range $0 < Q^2 < 11 \text{ GeV}^2$ in the present model. The enhancement of the double ratio for neutron R_n for $0 < Q^2 < 2 \text{ GeV}^2$ with $0.5\rho_0$ and ρ_0 , and the quenching for the proton R_p in symmetric nuclear matter, were also obtained in Ref. [99] by the covariant spectator quark model.

V. SUMMARY AND DISCUSSIONS

We have studied the nucleon electromagnetic (EM) form factors in symmetric nuclear matter as well as in vacuum, using a light-front motivated quark-spin coupling model with the one- and two-scale models of the nucleon wave functions. The in-medium inputs for the light-flavor up and down constituent quark properties are obtained by the quark-meson coupling model, which has proven to be very successful in describing the hadron and nuclear properties in medium based on the quark degrees of freedom.

We have found that the two-scale model nucleon wave functions describe well the nucleon EM form factors in vacuum. Our first prediction is that the zero of the proton EM form factor ratio (the zero of the proton electric form factor) in vacuum, to be about 15 GeV^2 .

Based on the two-scale model with the two parameter sets which can respectively reproduce the proton and neutron magnetic moments reasonably well, we have studied the zero of the proton EM form factor ratio in medium. By the results, our second prediction of this study is that, the zero of the bound proton, or proton in symmetric nuclear matter, shifts to a smaller Q^2 value than that in vacuum as nuclear matter density increases.

Using the same two-scale model with the same parameter sets, we have calculated the proton EM form factor double ratio, which were extracted in JLab experiments. The model with the parameter set I for nuclear matter density $0.3\rho_0$, and the parameter set II for nuclear matter density $0.15\rho_0$, are both able to describe well the JLab data. The results suggest that the description of the bound proton, or the in-medium proton EM form factor double ratio data, may be explained based on the internal structure change of the bound proton in a nuclear medium.

We have further calculated the neutron EM form factor double ratio in symmetric nuclear matter, corresponding to the proton case. Our results show that the neutron double ratio in symmetric nuclear matter is enhanced relative to that in vacuum, while for the proton it is quenched, as was theoretically predicted in Ref. [28]. This can give another interesting aspect to understand the in medium modification of the nucleon structure.

For the future prospects, we can also study the nucleon axial-vector form factor in a nuclear medium with the same model. Furthermore, we can extend the model to study the octet baryon electromagnetic and axial-vector form factors in vacuum, as well as those in a nuclear medium.

Acknowledgement

This work was partly supported by the Fundação de Amparo à Pesquisa do Estado de São Paulo (FAPESP), No. 2015/16295-5 (J.P.B.C.M.), and No. 2015/17234-0 (K.T.), and Conselho Nacional de Desenvolvimento Científico e Tecnológico (CNPq), No. 401322/2014-9, No. 308025/2015-6 (J.P.B.C.M.), No. 400826/2014-3, and No. 308088/2015-8 (K.T.) of Brazil.

Appendix A: Matrix elements of the microscopic current

The derivation of the matrix elements of the microscopic nucleon current operator composed by $J_{\beta N}^+$, $\beta = a, b, c, d$ of Eq. (7) in terms of the valence nucleon wave function follows closely Refs. [33]. They are represented by the diagrams in Fig. 1. The blobs in the figure represent the color anti-triplet coupling of a pair of quark fields in scalar-isoscalar ($\epsilon^{lmn}\bar{\Psi}_{(l)}i\tau_2\gamma_5\Psi_{(m)}^C$) from the effective Lagrangian of Eq. (1).

The integration over the minus-component of the momentum is performed to eliminate the relative light-front time in the intermediate state propagations [65–67]. This procedure allows to introduce the momentum component of the valence light-front wave function in the computation of form factors (see e.g., Ref. [66]).

The nucleon EM current J_N^+ derived from the effective Lagrangian has contribution from each photo-absorption amplitude given by the two-loop triangle diagrams of Figs. 1a to 1d.

The photon is absorbed by quark-3:

$$\begin{aligned} \langle s' | J_{aN}^+(q^2) | s \rangle &= -m_N^2 \langle N | \hat{Q}_q | N \rangle \text{Tr} [i\tau_2 (-i)\tau_2] \int \frac{d^4 k_1 d^4 k_2}{(2\pi)^8} \Lambda(k_i, p') \Lambda(k_i, p) \bar{u}(p', s') \\ &\quad \times S(k'_3) \gamma^+ S(k_3) u(p, s) \text{Tr} [S(k_2) \gamma^5 S_c(k_1) \gamma^5] , \end{aligned} \quad (\text{A1})$$

with $S(p) = \frac{1}{\not{p} - m + i\epsilon}$, and $S_c(p) = \left[\gamma^0 \gamma^2 \frac{1}{\not{p} - m + i\epsilon} \gamma^0 \gamma^2 \right]^T$ with T denoting transposition. The four-momentum of the virtual quark-3 after the photo-absorption process is $k'_3 = k_3 + q$. The matrix element of the quark charge operator in isospin space is $\langle N | \hat{Q}_q | N \rangle$. The function $\Lambda(k_i, p)$ is chosen to introduce the momentum part of the three-quark light-front wave function, after the integrations over k^- . The contribution to the EM current represented by Fig. 1b is given by:

$$\begin{aligned} \langle s' | J_{bN}^+(q^2) | s \rangle &= -m_N^2 \langle N | \hat{Q}_q | N \rangle \int \frac{d^4 k_1 d^4 k_2}{(2\pi)^8} \Lambda(k_i, p') \Lambda(k_i, p) \bar{u}(p', s') S(k'_3) \gamma^+ S(k_3) \\ &\quad \times \gamma^5 S_c(k_1) \gamma^5 S(k_2) u(p, s) . \end{aligned} \quad (\text{A2})$$

While the contribution to the EM current represented by Fig. 1c is given by:

$$\begin{aligned} \langle s' | J_{cN}^+(q^2) | s \rangle &= m_N^2 \langle N | \tau_2 \hat{Q}_q \tau_2 | N \rangle \int \frac{d^4 k_1 d^4 k_2}{(2\pi)^8} \Lambda(k_i, p') \Lambda(k_i, p) \bar{u}(p', s') S(k_1) \\ &\quad \times \gamma^5 S_c(k_3) \gamma^+ S_c(k'_3) \gamma^5 S(k_2) u(p, s) . \end{aligned} \quad (\text{A3})$$

Finally, the contribution to the EM current represented by Fig. 1d is given by:

$$\begin{aligned} \langle s' | J_{dN}^+(q^2) | s \rangle &= -m_N^2 \text{Tr} [\hat{Q}_q] \int \frac{d^4 k_1 d^4 k_2}{(2\pi)^8} \Lambda(k_i, p') \Lambda(k_i, p) \bar{u}(p', s') S(k_2) u(p, s) \\ &\quad \times \text{Tr} [\gamma^5 S(k'_3) \gamma^+ S(k_3) \gamma^5 S_c(k_1)] . \end{aligned} \quad (\text{A4})$$

The light-front coordinates are defined as $k^+ = k^0 + k^3$, $k^- = k^0 - k^3$, $\vec{k}_\perp = (k^1, k^2)$. In each term of the nucleon current, from J_{aN}^+ to J_{dN}^+ , the Cauchy integrations over k_1^- and k_2^- are performed. That means the on-mass-shell pole of the propagators for the spectator particles 1 and 2 of the photon absorption process are taken into account. In the Breit-frame with $q^+ = 0$, there is a maximal suppression of the light-front Z-diagrams in J^+ [66, 68]. Thus the components of the momentum k_1^+ and k_2^+ are bounded such that $0 < k_1^+ < p^+$ and $0 < k_2^+ < p^+ - k_1^+$. The four-dimensional integrations of Eqs. (A1) to (A4) are reduced to the three-dimensional ones on the null-plane.

After the integrations over the light-front energies the momentum part of the wave function is introduced into the microscopic matrix elements of the current by the substitution

[33, 66]:

$$\frac{1}{2(2\pi)^3} \frac{\Lambda(k_i, p)}{m_N^2 - M_0^2} \rightarrow \Psi(M_0^2) . \quad (\text{A5})$$

Further, the same momentum wave function is chosen all N-q coupling schemes for simplification. Note, that the mixed case, $\alpha = 1/2$ in Ref. [33] ($\alpha = 1$ is chosen for the present Lagrangian density of Eq. (1)), could have different momentum dependence for each spin coupling, however, we choose the same momentum functions just to keep contact to the Bakamjian-Thomas (BT) [107] approach.

The analytical integration of Eq. (A1) of the k^- components of the momenta yields:

$$\begin{aligned} \langle s' | J_{aN}^+(q^2) | s \rangle &= 2p^{+2} m_N^2 \langle N | \hat{Q}_q | N \rangle \int \frac{d^2 k_{1\perp} dk_1^+ d^2 k_{2\perp} dk_2^+}{k_1^+ k_2^+ k_3^{+2}} \theta(p^+ - k_1^+) \theta(p^+ - k_1^+ - k_2^+) \\ &\times \text{Tr} [(\not{k}_2 + m)(\not{k}_1 + m)] \bar{u}(p', s') (\not{k}'_3 + m) \gamma^+ (\not{k}_3 + m) u(p, s) \Psi(M_0'^2) \Psi(M_0^2) , \end{aligned} \quad (\text{A6})$$

where $k_1^2 = m^2$ and $k_2^2 = m^2$. The squared-mass of the free-three quarks is defined by:

$$M_0^2 = p^+ \left(\frac{k_{1\perp}^2 + m^2}{k_1^+} + \frac{k_{2\perp}^2 + m^2}{k_2^+} + \frac{k_{3\perp}^2 + m^2}{k_3^+} \right) - p_\perp^2 , \quad (\text{A7})$$

and $M_0'^2 = M_0^2(k_3 \rightarrow k'_3, \vec{p}_\perp \rightarrow \vec{p}'_\perp)$.

The other terms of the nucleon current, as given by Eqs. (A2)-(A4) are also integrated over the k^- momentum components of particles 1 and 2 following the same steps used to obtain Eq. (A6) from Eq. (A1):

$$\begin{aligned} \langle s' | J_{bN}^+(q^2) | s \rangle &= p^{+2} m_N^2 \langle N | \hat{Q}_q | N \rangle \int \frac{d^2 k_{1\perp} dk_1^+ d^2 k_{2\perp} dk_2^+}{k_1^+ k_2^+ k_3^{+2}} \theta(p^+ - k_1^+) \theta(p^+ - k_1^+ - k_2^+) \\ &\times \bar{u}(p', s') (\not{k}'_3 + m) \gamma^+ (\not{k}_3 + m) (\not{k}_1 + m) (\not{k}_2 + m) u(p, s) \Psi(M_0'^2) \Psi(M_0^2) , \end{aligned} \quad (\text{A8})$$

$$\begin{aligned} \langle s' | J_{cN}^+(q^2) | s \rangle &= p^{+2} \langle N | \tau_2 \hat{Q}_q \tau_2 | N \rangle \int \frac{d^2 k_{1\perp} dk_1^+ d^2 k_{2\perp} dk_2^+}{k_1^+ k_2^+ k_3^{+2}} \theta(p^+ - k_1^+) \theta(p^+ - k_1^+ - k_2^+) \\ &\times \bar{u}(p', s') (\not{k}_1 + m) (\not{k}_3 + m) \gamma^+ (\not{k}'_3 + m) (\not{k}_2 + m) u(p, s) \Psi(M_0'^2) \Psi(M_0^2) , \end{aligned} \quad (\text{A9})$$

$$\begin{aligned} \langle s' | J_{dN}^+(q^2) | s \rangle &= p^{+2} m_N^2 \text{Tr} [\hat{Q}_q] \int \frac{d^2 k_{1\perp} dk_1^+ d^2 k_{2\perp} dk_2^+}{k_1^+ k_2^+ k_3^{+2}} \theta(p^+ - k_1^+) \theta(p^+ - k_1^+ - k_2^+) \\ &\times \text{Tr} [(\not{k}'_3 + m) \gamma^+ (\not{k}_3 + m) (\not{k}_1 + m)] \bar{u}(p', s') (\not{k}_2 + m) u(p, s) \Psi(M_0'^2) \Psi(M_0^2) . \end{aligned} \quad (\text{A10})$$

The normalization is chosen such that the proton charge is unity.

[1] G. E. Brown and M. Rho, Phys. Rev. Lett. 66 (1991) 2720.

- [2] T. Hatsuda and S. H. Lee, Phys. Rev. C 46, no. 1 (1992) R34.
- [3] P. A. M. Guichon, Phys. Lett. B 200 (1988) 235.
- [4] For a review (and references therein including various groups), K. Saito, K. Tsushima and A. W. Thomas, Prog. Part. Nucl. Phys. 58 (2007) 1.
- [5] For a review, R. S. Hayano and T. Hatsuda, Rev. Mod. Phys. 82 (2010) 2949.
- [6] For a review, W. K. Brooks, S. Strauch and K. Tsushima, J. Phys. Conf. Ser. 299 (2011) 012011.
- [7] G. Krein, A. W. Thomas and K. Tsushima, arXiv:1706.02688 [hep-ph].
- [8] C. R. Allton, S. Ejiri, S. J. Hands, O. Kaczmarek, F. Karsch, E. Laermann, C. Schmidt and L. Scorzato, Phys. Rev. D66 (2002) 074507.
- [9] P. de Forcrand and O. Philipsen, Nucl. Phys. B673 (2003) 170.
- [10] T. Inoue *et al.* [HAL QCD Collaboration], Phys. Rev. C **91** (2015) no.1, 011001.
- [11] F. Winter, W. Detmold, A. S. Gambhir, K. Orginos, M. J. Savage, P. E. Shanahan and M. L. Wagman, Phys. Rev. D **96** (2017) no.9, 094512.
- [12] F. Cardarelli, E. Pace, G. Salme and S. Simula, Phys. Lett. B357 (1995) 267; Few Body Syst. Suppl. 8 (1995) 345.
- [13] W. R. B. de Araujo, J. P. B. C. de Melo and T. Frederico, Phys. Rev. C52 (1995) 2733.
- [14] A. Denig and G. Salme, Prog. Part. Nucl. Phys. 68 (2013) 113.
- [15] For a review, D. F. Geesaman, K. Saito and A. W. Thomas, Ann. Rev. Nucl. Part. Sci. 45 (1995) 337.
- [16] For a review and more complete references, O. Hen, G. A. Miller, E. Piasetzky and L. B. Weinstein, Rev. Mod. Phys. **89** (2017) no.4, 045002.
- [17] S. Strauch *et al.* [Jefferson Lab E93-049 Collaboration], Phys. Rev. Lett. 91 (2003) 052301.
- [18] S. Strauch [E93-049 Collaboration], Eur. Phys. J. A 19, no. S1 (2004) 153.
- [19] P. Lava, J. Ryckebusch, B. Van Overmeire and S. Strauch, Phys. Rev. C 71 (2005) 014605.
- [20] For a review and more complete references, J. T. Suhonen, Front. in Phys. **5** (2017) 55.
- [21] D. H. Lu, A. W. Thomas, K. Tsushima, A. G. Williams and K. Saito, Phys. Lett. B 417 (1988) 217.
- [22] D. H. Lu, K. Tsushima, A. W. Thomas, A. G. Williams and K. Saito, Phys. Rev. C 60 (1999) 068201.
- [23] T. Frederico, B. V. Carlson, R. A. Rego and M. S. Hussein, J. Phys. G 15 (1989) 297.

- [24] E. F. Batista, B. V. Carlson and T. Frederico, Nucl. Phys. A 697 (2002) 469.
- [25] W. R. B. de Araujo, E. F. Suisso, E. F. Batista, B. V. Carlson and T. Frederico, AIP Conf. Proc. 739 (2005) 464.
- [26] R. Schiavilla, O. Benhar, A. Kievsky, L. E. Marcucci and M. Viviani, Phys. Rev. Lett. 94 (2005) 072303.
- [27] X. Xing, J. Hu and H. Shen, Phys. Rev. C **94** (2016) no.4, 044308.
- [28] I. C. Cloët, G. A. Miller, E. Piasetzky and G. Ron, Phys. Rev. Lett. **103** (2009) 082301.
- [29] J. P. B. C. de Melo, K. Tsushima, B. El-Bennich, E. Rojas and T. Frederico, Phys. Rev. C 90 no.3 (2014) 035201.
- [30] J. P. B. C. de Melo, K. Tsushima and T. Frederico, AIP Conf. Proc. 1735 (2016) 080006.
- [31] J. P. B. C. de Melo, K. Tsushima and I. Ahmed, Phys. Lett. B 766 (2017) 125.
- [32] K. Tsushima and J. P. B. C. de Melo, Few Body Syst. 58 (2017) 85.
- [33] W. R. B. de Araújo, E. F. Suisso, T. Frederico, M. Beyer and H. J. Weber, Phys. Lett. B 478 (2000) 86;
E. F. Suisso, W. R. B. de Araújo, T. Frederico, M. Beyer and H. J. Weber, Nucl. Phys. A 694 (2001) 351.
- [34] W. R. B. de Araujo, T. Frederico, M. Beyer and H. J. Weber, Eur. Phys. J. A 29 (2006) 227.
- [35] E. F. Suisso, W. R. B. de Araujo, T. Frederico, M. Beyer and H. J. Weber, Nucl. Phys. A **694** (2001) 351.
- [36] W. R. B. de Araujo, T. Frederico, M. Beyer and H. J. Weber, Braz. J. Phys. 34 (2004) 251.
- [37] M. K. Jones et al.[Jefferson Lab Hall A collaboration], Phys. Rev. Lett. 84 (2000) 1398.
- [38] E. J. Brash, A. Koslov, Sh. Li and G. M. Huber, Phys. Rev. C 65 (R) (2002) 051001.
- [39] O. Gayou et al., Phys. Rev. Lett. 88 (2002) 092301.
- [40] V. Punjabi *et al.*, Phys. Rev. C 71 (2005) 055202; Erratum: [Phys. Rev. C 71 (2005) 069902].
- [41] G. Ron *et al.*, Phys. Rev. Lett. 99 (2007) 202002.
- [42] A. J. R. Puckett *et al.*, Phys. Rev. Lett. 104 (2010) 242301.
- [43] G. Ron *et al.* [Jefferson Lab Hall A Collaboration], Phys. Rev. C 84 (2011) 055204.
- [44] A. J. R. Puckett *et al.*, Phys. Rev. C 85 (2012) 045203.
- [45] J. P. B. C. de Melo, T. Frederico, E. Pace and G. Salmè, Nucl. Phys. A 707 (2002) 399.
- [46] H. -C. Pauli, Eur. Phys. J. C 7 (1998) 289; “DLCQ and the effective interactions in hadrons” in: New Directions in Quantum Chromodynamics, C.-R. Ji and D.P. Min, Editors, American

- Institute of Physics, (1999) 80-139.
- [47] T. Frederico and H. C. Pauli, Phys. Rev. D 64 (2001) 054007.
 - [48] T. Frederico, H. C. Pauli and S. G. Zhou, Phys. Rev. D 66 (2002) 054007; Phys. Rev. D 66 (2002) 116011.
 - [49] J. P. B. C. de Melo, T. Frederico, E. Pace and G. Salme, Phys. Lett. B 581 (2004) 75.
 - [50] J. P. B. C. de Melo, T. Frederico, E. Pace, and G. Salme, Phys. Rev. D 73 (2006) 074013.
 - [51] E. Pace, G. Salme, T. Frederico, S. Pisano and J. P. B. C. de Melo, Nucl. Phys. A 790 (2007) 606.
 - [52] J. P. B. C. de Melo, T. Frederico, E. Pace, S. Pisano and G. Salme, Phys. Lett. B 671 (2009) 153.
 - [53] E. Pace, J. P. B. C. de Melo, T. Frederico, S. Pisano and G. Salme, Nucl. Phys. Proc. Suppl. 199 (2010) 258.
 - [54] S. J. Brodsky, H.-C. Pauli and S. S. Pinsky, Phys. Rep. 301 (1998) 299.
 - [55] F. Iachello, N.C. Mukhpadhyay and L. Zang, Phys. Rev. D 44 (1991) 88.
 - [56] A. V. Anisovich, V. V. Anisovich and A. V. Sarantsev, Phys. Rev. D 62 (R) (2000) 051502.
 - [57] S. Godfrey and N. Isgur, Phys. Rev. D 32 (1985) 189.
 - [58] F. Cardarelli, I. L. Grach, I. M. Narodetskii, E. Pace, G. Salmè and S. Simula, Phys. Lett. B 332 (1994) 1;
F. Cardarelli, I.L. Grach, I.M. Narodetskii, G. Salmè and S. Simula, Phys. Lett. B 349 (1995) 393.
 - [59] H.-M. Choi and C.-R. Ji, Phys. Rev. D 59 (1999) 074015; D. Arndt and C.-R.Ji, *ibid.* 60 (1999) 094020.
 - [60] E. M. Aitala et al., Phys. Rev. Lett. 86 (2001) 4768.
 - [61] G. P. Lepage and S. J. Brodsky, Phys. Rev. D 22 (1980) 2157.
 - [62] S. J. Brodsky and F. Schlumpf, Phys. Lett. B 329 (1994) 111; Prog. Part. Nucl. Phys. 34 (1995) 69.
 - [63] F. Cardarelli and S. Simula, Phys. Rev. C 62 (2000) 065201; S. Simula, nucl-th/0105024.
 - [64] J. Carbonell, B. Desplanques, V. Karmanov and J.-F. Mathiot, Phys. Rep. 300 (1998) 215; and references therein.
 - [65] J. H. O. Sales, T. Frederico, B. V. Carlson and P. U. Sauer, Phys. Rev. C 61 (2000) 044003; Phys. Rev. C 63 (2001) 064003.
 - [66] T. Frederico and G. A. Miller, Phys. Rev. D 45 (1992) 4207.

- [67] For example (and references therein), C. R. Ji and D. P. Min, “QCD, light cone physics and hadron phenomenology”, Proceedings, 10th Nuclear Summer School and Symposium, NuSS’97, Seoul, Korea, June 23-28, 1997, Singapore, Singapore: World Scientific (1998) 273 p.
- [68] J. P. B. C. de Melo, H. W. Naus and T. Frederico, Phys. Rev. C 59 (1999) 2278.
- [69] B.L.G. Bakker, H.-M. Choi and C.-R. Ji, Phys. Rev. D 63 (2001) 074014.
- [70] P. L. Chung and F. Coester, Phys. Rev. D 44 (1991) 229.
- [71] W. R. B. de Araújo, T. Frederico, M. Beyer and H. J. Weber, J. Phys. G 25 (1999) 1589.
- [72] W. R. B. de Araújo, T. Frederico, M. Beyer and H. J. Weber, Eur. Phys. J. A 29 (2006) 227.
- [73] G. A. Miller, A. W. Thomas and S. Theberge, Phys. Lett. **91B** (1980) 192;
S. Theberge, A. W. Thomas and G. A. Miller, Phys. Rev. D **22** (1980) 2838 Erratum: [Phys. Rev. D **23** (1981) 2106];
A. W. Thomas, S. Theberge and G. A. Miller, Phys. Rev. D **24** (1981) 216;
- [74] A. W. Thomas, S. Theberge and G. A. Miller, Phys. Rev. D **24** (1981) 216.
- [75] I. C. Cloët, W. Bentz and A. W. Thomas, Phys. Rev. C **90** (2014) 045202.
- [76] C. Patrignani et al. (Particle Data Group), Chin. Phys. C, 40 (2016) 100001.
- [77] P. J. Mohr, D. B. Newell and B. N. Taylor, Rev. Mod. Phys. 88 no.3 (2016) 035009.
- [78] J. C. Bernauer *et al.* [A1 Collaboration], Phys. Rev. Lett. 105 (2010) 242001.
- [79] G. Salmé, T. Frederico and E. Pace, Few Body Syst. 56 no. 6-9 (2015) 303.
- [80] J. P. B. C. de Melo, T. Frederico, E. Pace, S. Pisano and G. Salme, Phys. Lett. B 671 (2009) 153.
- [81] G. Ramalho and K. Tsushima, Phys. Rev. D 84 (2011) 054014.
- [82] G. Holer et al., Nucl. Phys. B 144 (1976) (505) 505.
- [83] H. Y. Gao, Int. J. Mod. Phys. E 12 (2003) 1; Erratum: [Int. J. Mod. Phys. E 12 (2003) 567.
- [84] P. A. M. Guichon, K. Saito, E. N. Rodionov and A. W. Thomas, Nucl. Phys. A 601 (1996) 349;
K. Saito, K. Tsushima and A. W. Thomas, Nucl. Phys. A 609 (1996) 339;
Phys. Rev. C 55 (1997) 2637;
K. Tsushima, K. Saito, J. Haidenbauer and A. W. Thomas, Nucl. Phys. A 630 (1998) 691;
P. A. M. Guichon, A. W. Thomas and K. Tsushima, Nucl. Phys. A 814 (2008) 66.
- [85] P. G. Blunden and G. A. Miller, Phys. Rev. C **54** (1996) 359.

- [86] P. G. Blunden, M. Burkardt and G. A. Miller, Phys. Rev. C **59** (1999) R2998;
P. G. Blunden, M. Burkardt and G. A. Miller, Phys. Rev. C **60** (1999) 055211;
P. G. Blunden, M. Burkardt and G. A. Miller, Phys. Rev. C **61** (2000) 025206.
- [87] G. A. Miller and J. R. Smith, Phys. Rev. C **65** (2002) 015211 Erratum: [Phys. Rev. C **66** (2002) 049903].
- [88] W. Albrecht, H. J. Behrend, H. Dorner, W. Flauger and H. Hultschig, Phys. Lett. 26B (1968) 642.
- [89] S. Rock et al., Phys. Rev. Lett. 49 (1982) 1139.
- [90] E. E. W. Bruins *et al.*, Phys. Rev. Lett. 75 (1995) 21.
- [91] H. Anklin *et al.*, Phys. Lett. B 428 (1998) 248.
- [92] G. Kubon *et al.*, Phys. Lett. B 524 (2002) 26.
- [93] B. Anderson *et al.* [Jefferson Lab E95-001 Collaboration], Phys. Rev. C 75 (2007) 034003.
- [94] J. Lachniet *et al.* [CLAS Collaboration], Phys. Rev. Lett. 102 (2009) 192001.
- [95] B. D. Serot and J. D. Walecka, Adv. Nucl. Phys. 16 (1986) 1.
- [96] J. R. Stone, N. J. Stone and S. A. Moszkowski, Phys. Rev. C 89 (2014) 044316.
- [97] C. J. Horowitz and B. D. Serot, Nucl. Phys. A **399** (1983) 529.
- [98] D. H. Lu, A. W. Thomas, K. Tsushima, A. G. Williams and K. Saito, Phys. Lett. B 417 (1998) 217.
- [99] G. Ramalho, K. Tsushima and A. W. Thomas, J. Phys. G 40 (2013) 15102.
- [100] J. Arrington, W. Melnitchouk and J. A. Tjon, Phys. Rev. C 76 (2007) 035205.
- [101] M. Ostrick *et al.*, Phys. Rev. Lett. 83 (1999) 276;
C. Herberg *et al.*, Eur. Phys. J. A 5 (1999) 131;
D. I. Glazier *et al.*, Eur. Phys. J. A 24 (2005) 101.
- [102] I. Passchier *et al.*, Phys. Rev. Lett. 82 (1999) 4988.
- [103] T. Eden *et al.*, Phys. Rev. C 50 (1994) R1749.
- [104] H. Zhu *et al.* [E93026 Collaboration], Phys. Rev. Lett. 87 (2001) 081801;
R. Madey *et al.* [E93-038 Collaboration], Phys. Rev. Lett. 91 (2003) 122002;
G. Warren *et al.* [Jefferson Lab E93-026 Collaboration], Phys. Rev. Lett. 92 (2004) 042301.
- [105] S. Riordan *et al.*, Phys. Rev. Lett. 105 (2010) 262302.
- [106] R. Schiavilla and I. Sick, Phys. Rev. C 64 (2001) 041002.
- [107] B. Bakamjian and L. H. Thomas, Phys. Rev. 92 (1953) 1300.